AtSDR4L and paralog promote seed-to-seedling transition in multiple seed compartments

Bailan Lu*, Dongeun Go*, Jiayi Shan, Liang Song

Department of Botany, University of British Columbia, Vancouver, British Columbia V6T 1Z4, Canada

* These authors contributed equally to the work.

Author for correspondence: Liang Song

Email: liang.song@botany.ubc.ca

Abstract

Arabidopsis thaliana SEED DORMANCY 4-LIKE (AtSDR4L) and its paralog Dynamic Influencer of Gene Expression 2 (DIG2) act as transcriptional co-repressors to promote seed-to-seedling phase transition. Their regulatory roles at the temporal and tissue-specific scales remain elusive. Here, we show that *Atsdr4l dig2* seeds over-accumulate multiple hormones, and the mutant phenotypes are alleviated by abscisic acid (ABA) antagonists and gibberellin (GA). Dissected mutant embryos exhibit stunted growth due to reduced cell differentiation and expansion. The double mutant results in extensive changes in gene expression in both the seed coat and the embryo, including many transcription factors genes, with a subset of the genes differentially expressed tissue-specifically. Transcriptomes of *Atsdr4l-5 dig2* seed compartments form a distinct cluster from those of the mutant seedlings of *Atsdr4l* and Polycomb Repressive Complex (PRC)-related genes, suggesting developmental stage-specific role of these regulators. Together, these results demonstrated that AtSDR4L and DIG2 work in concert to launch the growth potential in the embryo and alleviate the constraints in the seed coat to prepare seeds for germination.

Key words

AtSDR4L, DIG2, embryo, seed coat, ABA, auxin, seed compartment transcriptome, seed-to-seedling transition

Introduction

Seed-to-seedling transition involves break of dormancy, germination, and seedling establishment. During seed maturation, dormancy is acquired to prevent germination in otherwise favorable conditions. Being an adaptive trait, dormancy reflects the interplay between genetic and environmental factors. The strength and types of the dormancy vary by species, ecotypes, and are influenced by environmental cues such as temperature, light, and nitrate (Baskin and Baskin, 2004; Iwasaki *et al.*, 2022; Sajeev *et al.*, 2024). Physiological dormancy is the best studied among five main types of seed dormancy (Baskin and Baskin, 2020). Arabidopsis seeds have non-deep physiological dormancy, characterized by a fully developed embryo and the ability to break dormancy through dry storage (after-ripening). Arabidopsis seed coat, including both the testa and the endosperm, plays important roles in dormancy (Debeaujon *et al.*, 2000; Finch-Savage and Leubner-Metzger, 2006). Removal of the seed coat or the endosperm de-arrest embryo growth (Bethke *et al.*, 2007; Lee *et al.*, 2010).

Dormancy in Arabidopsis is maintained by high abscisic acid (ABA) levels upon imbibition as well as ABA-independent mechanisms (Iwasaki *et al.*, 2022), whereas germination is promoted by elevated ratio of gibberellins (GA) to ABA (Kucera *et al.*, 2005). The level of ABA is the outcome of ABA biosynthesis and inactivation. Several *9-cis-epoxycarotenoid dioxygenase* (*NCED*) genes, encoding enzymes that catalyze a committed step of ABA biosynthesis, are expressed with comprehensive spatiotemporal specificity in various compartments of developing and maturing seeds (Tan *et al.*, 2003; Lefebvre *et al.*, 2006; Frey *et al.*, 2012). The level of CYP707A2, a key enzyme for ABA catabolism, increases rapidly upon imbibition (Kushiro *et al.*, 2004). Single mutant of *cyp707a2* and its higher-order mutants with other ABA 8-hydroxylases such as *cyp707a1* and *cyp707a3* over-accumulate ABA and are more dormant (Okamoto *et al.*, 2006). Furthermore, the distribution of ABA in seeds is also determined by transport from the endosperm to the embryo by ABC transporters (Kang *et al.*, 2015). GA level is low in dry seeds and increases by cold stratification or imbibition (Weitbrecht *et al.*, 2011). Increase in GA enables cell wall loosening in both the endosperm and the embryo, and promotes elongation of the lower hypocotyl. Consequently, the rupture of the endosperm and protrusion of the radical complete germination. Many other hormones, such as auxin, ethylene, jasmonates, and brassinosteroids modulate the balance between ABA and GA through crosstalk at the hormone biosynthesis and signaling steps to regulate the transition from seed to seedlings (Gazzarrini and Tsai, 2015; Skubacz and Daszkowska-Golec, 2017). Regulators such as DELAY OF GERMINATION 1 (DOG1), MOTHER OF FT AND TFL1 (MFT), ABA INSENSITIVE5 (*ABI5*), and RGA-LIKE 2 (RGL2) integrate light, temperature, and hormonal cues to modulate dormancy (Graeber *et al.*, 2014; Yang *et al.*, 2020*a*).

Arabidopsis SEED DORMANCY 4-LIKE (*AtSDR4L*) encodes a transcriptional co-repressor that promotes seed-to-seedling transition (Cao *et al.*, 2020; Liu *et al.*, 2020; Wu *et al.*, 2022; Zheng *et al.*, 2022). AtSDR4L physically interacts with Polycomb Repressive Complex (PRC)-interacting transcription factor (TF) VIVIPAROUS1/ABI3-LIKE2 (VAL2) (Lu *et al.*, 2024). AtSDR4L and VAL2 bind to the upstream of *LEAFY COTYLEDON1* (*LEC1*), *ABA INSENSITIVE3* (*ABI3*), its own gene and a few *AtSDR4L* paralogs. The binding is often

associated with reduced level of repressive histone mark H3K27me3 at these loci. LEC1, ABI3, along with FUSCA3 (FUS3), and LEC2, are collectively known as LAFL master TFs that regulate seed development and their expression need to be turned off during seed-to-seedling transition (Gazzarrini and Song, 2024). All *LAFL* genes are de-repressed in *Atsdr4l* loss-of-function seedlings (Wu *et al.*, 2022; Zheng *et al.*, 2022). Defects in seed-to-seedling transition are exacerbated when both *AtSDR4L* and its paralogs are mutated, exhibiting severe seed dormancy and extensive accumulation of seed storage compounds in seedlings (Zheng *et al.*, 2022). The molecular mechanism of strong seed dormancy has been attributed to elevated expression of *NCED* (Liu *et al.*, 2020; Zheng *et al.*, 2022). However, tissue-specific regulation of dormancy in the *Atsdr4l* mutants and control of dormancy by epigenetic regulators haven't been fully elucidated.

In this study, we examined how AtSDR4L and paralogs promote the break of dormancy and subsequent seed-to-seedling transition in the seed coat and the embryo by comprehensive hormone analysis, seed compartment-specific transcriptome profiling, and physiological assays. We revealed an extensive and sophisticated interplay between hormones and TFs, and provided potential mechanistic links to explain the inhibited cell differentiation and growth in the embryonic axis of *Atsdr4l dig2*.

Results

Atsdr4l dig2 phenotypes are attenuated by ABA antagonists

Previously, multiple groups have shown that *Atsdr4l* single and higher-order mutants exhibited delayed seed germination and defective seedling establishment (Cao *et al.*, 2020; Liu *et al.*, 2020; Wu *et al.*, 2022; Zheng *et al.*, 2022). We crossed *Atsdr4l-5*, a CRISPR/Cas9 segmental deletion line of *AtSDR4L* (Lu *et al.*, 2024) with T-DNA insertion lines of *DIG* genes (Fig. S1). Consistently with a previous study (Zheng *et al.*, 2022), *Atsdr4l-5 dig2* seeds are more dormant than the single mutant, and storage lipids accumulate ectopically in *Atsdr4l-5 dig2* seedlings (Fig. 1A-C, S1). Therefore, we focus on *Atsdr4l-5 dig2* in this study to examine the temporal and spatial regulation of seed-to-seedling transition by AtSDR4L and its paralogs.

Because ABA is a strong inhibitor of germination, we germinated wild-type and mutant seeds on plates supplemented with ABA antagonist antabactin (Vaidya *et al.*, 2021) or antagonist / agonist ABA1019, formerly known as compound 7 (Diddi *et al.*, 2021). At 50 μM, both compounds promote germination of *Atsdr4l-5* single and double mutants (Fig. 1A, 1C, S1). Since freshly harvested *Atsdr4l* seeds were reported to be unresponsive to GA (Cao *et al.*, 2020), we applied GA in the germination assays with or without ABA analogues. Our results confirmed that GA alone on briefly after-ripened *Atsdr4l-5 dig2* seeds barely releases the strong dormancy (Fig. 1A, S1). In contrast, including GA in ABA antagonist treatment further improves seed germination, promotes embryo axis elongation, and alleviates the severity of the embryonic traits (Fig.1A-C). These results suggest that ABA plays a primary role in the dormancy of *Atsdr4l-5 dig2*.

Multiple phytohormones are mis-regulated in *Atsdr4l dig2* seeds

Previously, Zheng *et al.* showed that dry seeds of *Atsdr4l dig2* (known as *sfl1 sfl4* in their study) contain more ABA and auxin (Zheng *et al.*, 2022). Consistently, we also observed that ABA and indole-3-acetic acid (IAA) levels in *Atsdr4l-5 dig2* seeds are 4.1 times and 1.9 times as much as those in wild-type Col-0 seeds, respectively (Fig. 2). Elevated levels of ABA and auxin in *Atsdr4l dig2* corroborate the double mutant's delayed germination. Furthermore, we found that dry seeds of *Atsdr4l-5 dig2* over-accumulate oxidized (7'-OH ABA, DPA) and conjugated (ABAGE, IAA-Asp, IAA-Glu) forms of ABA and auxin, suggesting that the deactivation pathways of ABA and auxin are up-regulated in *Atsdr4l dig2* seeds, presumably in response to the high levels of active hormones.

Surprisingly, we observed a strong over-accumulation of 1-aminocyclopropane-1-carboxylic acid (ACC) (Fig. 2), the immediate precursor of ethylene. Because ethylene is known to break dormancy (Ahammed *et al.*, 2020), the effect of ACC overaccumulation might be masked by ABA in the germination of *Atsdr4l-5 dig2*. Additionally, the level of cis-zeatin riboside (c-ZR) in *Atsdr4l dig2* is almost three times as high as in Col-0 seeds (Fig. 2). Unlike trans-zeatin-type cytokinins, cis-zeatin and cZR are often considered less biologically active and are more abundant in growth-limiting tissues (Gajdošová *et al.*, 2011; Schäfer *et al.*, 2015). Although unlike the aforementioned hormones, the increase in c-ZR is statistically insignificant ($P > 0.05$, two-tailed Student's t-test), the trend is consistent with the reduced growth potential of the double mutant.

Dormancy in *Atsdr4l dig2* is contributed by both the embryo and the seed coat

Because hormones regulate germination through both the endosperm and the embryo, we carried out a seed coat bedding assay (SCBA) (Lee *et al.*, 2010) to determine the tissue of origin for the strong dormancy of *Atsdr4l-5 dig2*. In the SCBA, dissected wild-type Col-0 and mutant embryos were placed on either Col-0 or mutant seed coat that contains the testa and the endosperm. We observed a clear difference between Col-0 and *Atsdr4l-5* single or double mutant since 2 days after imbibition (DAI) (Fig. S2). By 3DAI, Col-0 embryos on all bedding strata and intact seeds were almost fully established as marked by expanded green cotyledons, elongated hypocotyls and roots with collet hairs whereas *Atsdr4l-5* single mutant was established at a slower rate than Col-0 (Fig. 3A). By contrast, the majority of isolated *Atsdr4l-5 dig2* embryos remained arrested for axis elongation and collet hair development; cotyledon expansion and greening were very subtle and less synchronized (Fig. 3B). These defects were attenuated when the double mutant was complemented with native promoter-driven *DIG2* or *AtSDR4L* (Fig. S2C). Collectively, these results reveal that the embryos of *Atsdr4l-5* and *Atsdr4l-5 dig2* contribute substantially to the enhanced dormancy. Seedling establishment in intact seeds is slower than corresponding dissected embryos in all genotypes, confirming the positive regulation of dormancy by the seed coat (Fig. 3, S2). Additionally, seedling establishment in a few lines of *Atsdr4l-5 dig2* is further delayed when dissected embryos were placed on *Atsdr4l-5 dig2* seed coat (first two biological replicates in Fig. 3B), suggesting that (1) *Atsdr4l-5 dig2* endosperm produces a higher level of inhibitory substances, presumably ABA,

and / or (2) *Atsdr4l-5 dig2* embryo is hypersensitive to the inhibition originated from the mutant endosperm.

Atsdr4l dig2 embryo is more sensitive to osmotic stress and ABA

To examine whether *Atsdr4l-5 dig2* embryo has elevated sensitivity to ABA, we compared the growth of dissected wild-type and mutant embryos in the presence of 300 mM D-mannitol and 0.1 μM ABA (Fig. 4). On mock plates, approximately a third of *Atsdr4l-5 dig2* embryos lacked collet hairs, contrastingly to the presence of collet hairs in all of Col-0, *Atsdr4l-5*, and *Atsdr4l-5 dig1* embryos. All mutant lines exhibited more severely arrested seedling establishment in response to osmotic stress or ABA. Additionally, fewer *Atsdr4l-5* and *Atsdr4l-5 dig1* embryos developed collet hairs than Col-0 while there was no collet hair growth in any *Atsdr4l-5 dig2* embryos. Thus, *AtSDR4L* synergistically works with its paralogs, in particular *DIG2*, to reduce embryo's sensitivity to ABA and osmotic stress and facilitate the phase transition from seed to seedlings. We also examined dissected embryos' response to ABA analogues. Interestingly, growth of Col-0, *Atsdr4l-5*, and *Atsdr4l-5 dig2* embryo was completely inhibited by ABA1019 (Fig. S3), whereas germination of corresponding mutant seeds was promoted by ABA1019 (Fig. 1A, 1C, S1C), thereby indicating tissue-specific response to certain ABA analogues.

Atsdr4l dig2 embryo and seed coat show both similar and unique misregulation of genes

The physiological changes in seeds and early seedlings of *Atsdr4l-5 dig2* prompted us to examine the transcriptomes of seed compartments in wild-type and the double mutant. We prepared RNA-seq libraries using dissected seed coats and the embryos of Col-0 and *Atsdr4l dig2*. Hierarchical clustering reveals that the tissue type and genotype contribute to most differences between the samples (Fig. S5A). The drastic difference in the expression of endosperm marker *EARLY-PHYTOCHROME-RESPONSIVE1* (*EPR1*) between the embryo and the seed coat samples indicates clear separation of the tissues (Fig. 5A) (Dubreucq *et al.*, 2000). *AtSDR4L* is up-regulated in both mutant tissues, confirming previously reported self-repression (Wu *et al.*, 2022; Lu *et al.*, 2024). Several key regulators of seed maturation are de-repressed in the embryo and / or the seed coat of *Atsdr4l-5 dig2* (Fig. 5A). Notably, the basal expression level and the extent of up-regulation are locus- and compartment-specific. *ABI3* transcript is more abundant in the embryo, whereas *FUS3* transcript is more abundant in the seed coat of wild-type samples. The tissue preference of these two genes remains after being de-repressed in *Atsdr4l-5 dig2*. *MFT* and *DOG1* have comparable basal levels of expression between the two compartments, but *MFT* is only significantly up-regulated in *Atsdr4l dig2* embryo, whereas *DOG1* is significantly up-regulated in both mutant tissues, with a stronger induction in the seed coat. The two seed compartments share 2795 and 2110 significantly up-regulated and down-regulated genes, respectively (Fig. 5B). The magnitude of differential expression is significantly and positively (Pearson correlation coefficient = 0.91, $p < 2.2 \times 10^{-16}$) correlated between the two tissues (Fig. 5C). Consistent with delayed germination and lipid overaccumulation, genes related to positive regulation of dormancy and seed storage reserve accumulation have significantly elevated expression in the mutant embryo and seed coat (Fig. 5C). The upregulated genes in both tissues are enriched for biological processes related to the

responses to hormonal, chemical and abiotic signals (Fig. 5D), with a subset of the genes showing embryo-specific functions (Fig. S5C). The down-regulated targets in both tissues are associated with responses to chemical and biotic stimuli, while those in embryo also have relations to cell wall modification, transcription and metabolic processes, and those in endosperm are linked with defense and toxin responses (Fig. 5D). Specifically, genes encoding ABA signaling components, including *PYR/PYL* receptors, *PP2C*s, and *SnRK2*s, as well as auxin-related *AIL* family members exhibit either elevated or reduced expression in both seed compartments in *Atsdr4l-5 dig2* mutant (Fig. 5C, S5B). Collectively, the RNA-seq results showed that a large number of genes are mis-regulated in *Atsdr4l-5 dig2*, and several key developmental or hormonal regulators are specifically or more profoundly regulated in one of the seed compartments.

Atsdr4l dig2 embryo exhibits delayed axis elongation and differentiation during seedling establishment

A large number of TFs are misregulated in the seed compartments of *Atsdr4l-5 dig2*. We observed that that *LONESOME HIGHWAY* (*LHW*), encoding a regulator of protoxylem differentiation (Ohashi-Ito and Bergmann, 2007; Ohashi-Ito *et al.*, 2013), is strongly down-regulated in *Atsdr4l-5 dig2* embryo (Fig. 6A). Germination is promoted by mechanical signals from the elongation of the axis, in particular the cell expansion at the hypocotyl-radicle junction (Sliwinska *et al.*, 2009; Bassel *et al.*, 2014). *Atsdr4l* seedlings exhibit condition-dependent, partial penetrance of pleiotropic defects in seed-to-seedling transition, and stunted growth in the lower hypocotyl is one of the most consistent traits (Wu *et al.*, 2022). Therefore, we examined whether cell differentiation and expansion is affected in this region to prevent *Atsdr4l dig2* seeds from completing germination. Col-0 and *Atsdr4l-5 dig2* embryos at 2 DAI were stained by the periodic acid-propidium iodide (PA-PI) method (Truernit *et al.*, 2008). We confirmed the lack of collet hair and observed smaller cell size in the *Atsdr4l-5 dig2* seedlings (Fig. 6B-C, S4). Consistent with the down-regulation of *LHW*, protoxylem starts to appear in the vascular tissue of Col-0 seedlings, whereas the corresponding tissue in *Atsdr4l dig2* remains undifferentiated (Fig. 6B, S4), possibly permitting more obvious developmental differences between wild type and the mutant at later stages.

Transcriptome changes in *Atsdr4l dig2* seeds lay the groundwork for altered developmental path in seedlings

To examine the genes regulated by AtSDR4L in seeds versus later developmental stages, we compared *Atsdr4l-5 dig2* seed compartment transcriptome with public seedling transcriptomes of *Atsdr4l* and other epigenetic mutants that are phenotypically similar (Go *et al.*, 2024). Clustering of the RNA-seq data shows that *Atsdr4l* seedling transcriptome is highly similar to *pkl*, *val1 val2*, *clf28 swn7*, *ring1a ring1b* and *bmi1a bmi1b bmi1c* (Fig. 7A). By contrast, *Atsdr4l-5 dig2* embryo and seed coat form a distinct cluster (Fig. 7A). Grouping of the differentially expressed genes by $\log_2$ fold changes identifies one cluster of genes with common and strong up-regulation in *Atsdr4l* single mutants and the selected *prc* mutants, while the magnitudes of de-repression are modest in the double mutant seed compartments (Fig. 7B-C). This group

includes master TFs of seed maturation *ABI3* and *FUS3*, and a number of seed storage proteins. Intriguingly, a subset of the genes exhibit opposite trends of misregulation between the double mutant seed compartment(s) and *Atsdr4l* seedlings, including *AGL15*, *NF-YC4* and a subset of the *AINTEGUMENTA-LIKE* (*AIL*) members (Fig. 7C), implying the potential stage-specific functions of AtSDR4L. Some of the genes involved in auxin biosynthesis and embryogenesis, such as *YUCCA2* (*YUC2*), *AIL5* and *BABY BOOM* (*BBM*), also exhibit increased expression in both *Atsdr4l dig2* seed and *Atsdr4l* seedlings (Fig. 7D). *AIL5* and *BBM* are predominantly expressed in *Atsdr4l dig2* embryo and exhibit upregulation in both compartments. On the other hand, the master TFs of embryogenesis *LEC1*, *LEC2*, and *AGL15* are only significantly up-regulated in the single mutant seedlings but not in double mutant seeds, suggesting that *BBM* and *AIL5* act upstream to induce these pluripotent genes in *Atsdr4l-5 dig2*. The distribution of *ABI5* and *ABI4* transcripts differs drastically between the seed tissues and the seedlings, and *ABI5* shows weak up-regulation in both seed compartments of *Atsdr4l-5 dig2*, while *ABI4* is specifically expressed in the embryo and is not differentially expressed in the mutant (Fig. 7D). Combined, these data suggest sequential actions of AtSDR4L and its paralog DIG2 to modulate gene expression in seeds, sometimes in a tissue-specific manner, to prevent massive expression of seed maturation genes in seedlings.

Discussions

Hormonal and gene expression changes in seed compartments promote dormancy of *Atsdr4l dig2*

Arabidopsis seeds have non-deep physiological dormancy, and the balance between dormancy and germination is fine-tuned by phytohormones (Finch-Savage and Leubner-Metzger, 2006; Penfield, 2017). The results from germination assays and hormone quantification supported that the rising amount of endogenous ABA correlates with the enhanced dormancy in *Atsdr4l-5 dig2* seeds (Fig. 1, 2). ABA antagonist treatments further confirmed that ABA is the major determinant for inhibited germination and subsequent seedling establishment in *Atsdr4l-5 dig2*. The defects in germination, embryonic traits, and axis elongation of intact *Atsdr4l-5 dig2* seeds are alleviated by antabactin and ABA1019 (Fig. 1, S1B). Contrastingly, ABA1019 completely suppressed the growth of dissected Col-0 and mutant embryos (Fig. S3). Such differences in ABA1019's effects on intact seeds and dissected embryos could be dose- or tissue-dependent, and ABA1019 was reported to function as both an antagonist and agonist (Diddi *et al.*, 2021). Previous studies reported the opposing effects from the ligand-receptor interaction in which PYL2-bound pyrabactin acts as an ABA antagonist, whereas PYL1- or PYR1-bound pyrabactin functions as an agonist (Peterson *et al.*, 2010; Yang *et al.*, 2020*b*). Our transcriptome analysis showed that components of ABA signaling pathways exhibit common and unique differential expression in *Atsdr4l-5 dig2* embryo and the seed coat (Fig. S5). Among the *PYL*/*PYR* receptor genes, *PYL1*, which is known to express in the embryonic axis and at a lesser degree in the endosperm (Gonzalez-Guzman *et al.*, 2012), is specifically down-regulated in *Atsdr4l-5 dig2* embryo (Fig. S5). *PYR1* is commonly down-regulated in both compartments of *Atsdr4l-5 dig2* seeds, whereas *PYL8* is specifically up-regulated in the mutant embryo (Fig. S5). As such, we speculate that the opposite effect of ABA1019 on whole seeds and dissected embryos might be

contributed by the receptor-specific mode of actions and by the differences in the expression of various ABA receptors in seed coat and the embryo (Gonzalez-Guzman *et al.*, 2012). Previous study has shown that GFP-fused SnRK2.2 and SnRK2.6 were localized in developing embryos, and their expression in the endosperm was not addressed (Nakashima *et al.*, 2009). Our transcriptome data showed that *SnRK2.2* is specifically induced in the mutant embryo whereas *SnRK2.6* is solely repressed in the mutant seed coat (Fig. S5). ABA-responsive regulators such as *ABI3*, *ABI5*, and *DOG1* are up-regulated in both seed compartments of *Atsdr4l-5 dig2*, and *ABI3* and *MFT* transcripts accumulate to a higher abundance in the embryo than the seed coat (Fig. 5A). The transcriptomes also corroborate the observation that *Atsdr4l-5 dig2* seeds contain elevated levels of ABA and its oxidized or conjugated metabolites (Fig. 2). The ABA biosynthetic genes *NCED6* and *NCED3* are up-regulated in both seed compartments (Fig. 6A), consistent with the past findings in *Atsdr4l-5* single and higher-order mutants (Liu *et al.*, 2020; Zheng *et al.*, 2022). The higher abundance of the oxidized ABA metabolites (7'-OH ABA, DPA) may be explained by the up-regulation of the catabolic gene *CYP707A2* in the embryo (Fig. 5A) (Nambara and Marion-Poll, 2005; Nambara *et al.*, 2010; Bai *et al.*, 2022). Collectively, gene expression profiling supports the increased responsiveness to ABA in *Atsdr4l dig2* seeds. Preferential up-regulation of many positive regulators of ABA signaling is consistent with the SCBA results that *Atsdr4l-5 dig2* embryo is dormant even in the absence of the seed coat (Fig. 3).

Changes in other hormones are supported by the transcriptome data. *Atsdr4l-5 dig2* seeds over-accumulate IAA and its amino acid conjugates (Fig. 2). In Arabidopsis, IAA is synthesized via multiple tryptophan-dependent and independent pathways, and the conversion to IAA from indole-3-pyruvic acid, indole-3-acetamide, and indole-3-acetonitrile are catalyzed by YUC, AMIDASE 1 (AMI1), and NITRILASE (NIT) enzymes, respectively (Mano and Nemoto, 2012). Although most *YUC* genes were not detected in our samples, *YUC2* is significantly elevated in both the embryo and seed coat of *Atsdr4l-5 dig2*. Additionally, *NIT1*, *NIT2*, and *AMI1* are up-regulated in *Atsdr4l-2 dig2* embryo, suggesting that multiple pathways are activated in the mutant embryo to increase IAA biosynthesis. Thus, the enhanced dormancy of *Atsdr4l-5 dig2* embryo could result from elevated auxin level and the crosstalk between auxin and ABA to maintain an embryonic state (Belin *et al.*, 2009).

Although we did not detect GA in the hormone measurement, possibly due to the low level of GA in mature seeds (Weitbrecht *et al.*, 2011), transcriptome data revealed the up-regulation of GA catabolic gene *GA2ox6* and two DELLA genes, *RGL2* and *RGL3* (Fig. 5C), which may leverage the ABA-to-GA balance to promote dormancy (Piskurewicz *et al.*, 2008; Stamm *et al.*, 2012; Liu *et al.*, 2016). Additionally, GA-responsive expansin gene *EXP8* is weakly expressed in Col-0 seeds, especially in the seed coat, possibly because the brief imbibition during seed dissection activates *EXP8* (Fig. 7D). *EXP8* is virtually absent in *Atsdr4l-5 dig2* seeds, suggesting a low level of GA and delayed cell wall loosening (Weitbrecht *et al.*, 2011; Stamm *et al.*, 2012; Samalova *et al.*, 2023). This imbalance caused by altered ABA and GA signal transduction cascades may in part explain the need of ABA antagonists in combination with GA to break the enhanced dormancy in *Atsdr4l-5 dig2* mutant seeds.

Ethylene breaks dormancy and promotes germination through hormone crosstalk (Beaudoin *et al.*, 2000; Ghassemian *et al.*, 2000) and through repression of ethylene receptor ETR1 and subsequent de-repression of *ETHYLENE RESPONSE FACTOR12* (*ERF12*), the encoded TF of which recruits transcriptional co-repressor TOPLESS (TPL) to repress *DOG1* (Li *et al.*, 2019). The surprising increase in ethylene precursor ACC in *Atsdr4l-5 dig2* seeds (Fig. 2) might be indirectly induced by auxin. Previous studies have shown that ethylene synthesis may be stimulated by auxin in mungbean and pea (Yang and Hoffman), and Arabidopsis *ACC SYNTHASE* (*ACS*) expression can be induced by exogenous auxin treatments (Yamagami *et al.*, 2003; Tsuchisaka and Theologis, 2004). Our RNA-seq results showed increased expression of *ACS2* in the embryo and seed coat of *Atsdr4l-5 dig2*. However, the increase in *ERF12* transcript is very modest (< 1.5 fold) in *Atsdr4l-5 dig2* seeds, suggesting the rise in ethylene level in mutant seeds might not strongly affect dormancy in the presence of ABA and auxin. Our findings show that AtSDR4L and DIG2 regulate hormone signaling genes at the tissue-specific context in mature seeds.

AtSDR4L and DIG2 facilitate seedling establishment by promoting cell differentiation and repressing pluripotent genes

Atsdr4l-5 dig2 seedlings exhibit multiple developmental abnormalities post-germination. *Atsdr4l* single and higher-order mutants have fewer collet hairs, which is further reduced by stress treatments by ABA and osmolyte (Fig. 4). Consistent with reduced collet hair emergence and downregulation of *LHW*, a TF regulating protoxylem differentiation, in *Atsdr4l-5 dig2* (Fig. 6A), PA-PI-staining revealed that *Atsdr4l-5 dig2* but not wild-type seedlings lack protoxylem at 2 DAI (Fig. 6B). The regulation of axis growth by AtSDR4L and DIG2 may also involve *MFT*. *MFT* expression in the collet zone can be induced by ABA in imbibed seeds (Xi *et al.*, 2010). Because *Atsdr4l dig2* seeds over-accumulate ABA, the elevation of *MFT* transcript in the mutant embryo might be from the collet zone.

Transcriptome analysis indicates that AtSDR4L and DIG2 help to lower the accumulation of TFs promoting embryogenesis in the embryo compartment of mature seeds. The AIL family of TFs are important regulators of cell proliferation, meristem maintenance, and embryogenesis (Horstman *et al.*, 2014). Two *AIL* genes, *AIL2*/*BBM* and *AIL5* are commonly up-regulated between the two seed compartments of *Atsdr4l-5 dig2* (Fig. 5C), and the expression level of *BBM* is considerably higher in the embryo than in the seed coat (Fig. 7D). Up-regulation of *BBM* and *AIL5* is consistent between *Atsdr4l-5 dig2* seeds and *Atsdr4l* seedlings (Fig. 7C). BBM regulates early embryo development by transcriptionally activating *LAFL* (Boutilier *et al.*, 2002; Horstman *et al.*, 2017; Chen *et al.*, 2022). *AIL5* up-regulation may also be involved in the germination and embryonic phenotype, as its over-expressor is known to be hypersensitive to ABA during seed germination (Yano *et al.*, 2009), and cause overproliferation of somatic embryos and increased transcript abundance of seed maturation genes (Tsuwamoto *et al.*, 2010).Thus, restricting the expression of these *AIL* genes at a low level in the embryo at the end of seed maturation will favor seedling establishment over somatic embryogenesis post germination. Similarly, *FUS3* transcript abundance in mature wild-type seeds is low and the expression is largely confined to the seed coat. The up-regulation of *FUS3* in the embryo and the seed coat of *Atsdr4l-2 dig2*, along with *ABI3*, *DOG1*, *ABI5*, and *MFT*, likely explain the

stronger dormancy of the mutant seeds (Nakabayashi *et al.*, 2012; Dekkers *et al.*, 2016; Carrillo-Barral *et al.*, 2020; Alizadeh *et al.*, 2021). Since auxin and ABA promote seed maturation pathways and somatic embryogenesis in germinating seeds (Chen *et al.*, 2021), up-regulation of *FUS3* along with a high level of auxin and ABA in *Atsdr4l-2 dig2* seeds are likely to contribute to the embryonic traits observed in the mutant seedlings, which can be attenuated by treatment of ABA antagonists (Fig. 1B).

During seedling establishment, seed maturation genes are silenced by PRCs, and mutant seedlings of PRC core components and associated proteins exhibit a plethora of embryonic characteristics (Ogas *et al.*, 1997; Tsukagoshi *et al.*, 2007; Yang *et al.*, 2013; Go *et al.*, 2024). AtSDR4L and paralogs may repress the expression of *LAFL* TFs through PRCs because they bind to the upstream regions of *ABI3* and *LEC1*, physically interact with VAL2, and the H3K27me3 level of *ABI3* is reduced in 3-day-old *Atsdr4l* seedlings (Wu *et al.*, 2022; Lu *et al.*, 2024). The link to PRCs is further strengthened by the striking transcriptomic similarity between mutant seedlings of *Atsdr4l* and PRC components (Fig. 7A). Although AtSDR4L and paralogs accumulate to high levels in nearly matured and dry seeds, PRC2 core components and VAL2 are poorly expressed at these stages (Gazzarrini and Song, 2024). This imbalance may explain the low level of H3K27me3 at *ABI3* locus and the ABA-inducibility of *ABI3* in mature and germinating seeds. By contrast, H3K27me3 level is high at *LEC1* and *LEC2* loci in mature seeds, thus these genes are difficult to activate in wild-type seedlings. In *Atsdr4l* single and higher-order mutants, altered hormonal environment and up-regulation of TFs such as *BBM*, *FUS*, and *ABI3* in the embryo may facilitate the reactivation of *LEC1*, *LEC2*, and *AGL15* in seedlings, thus changing the cell fate and developmental trajectory of mutant seedlings (Fig. 8).

Taken together, we provide new insights into AtSDR4L and paralogs' role in the transition from seed to seedlings through comprehensive analyses of hormones and seed compartment-specific physiological assays and transcriptome profiles. The data add new information of PRC-related transcriptional regulation at important yet understudied developmental stages and tissues, and reveal potential mechanistic explanation for the stunted axis differentiation and growth in *Atsdr4l* single and higher-order mutants.

Materials and Methods

Plant materials and growth conditions

To generate the double mutants of *Atsdr4l-5* with T-DNA insertional mutants *dig1* (SALK_128578) and *dig2* (SALK_057406), the CRISPR deletion mutant *Atsdr4l-5* (Lu *et al.*, 2024) was crossed with *dig1 dig2* double mutant. *Atsdr4l-5 dig2* and *Atsdr4l-5 dig1* were segregated from F3 progeny of the cross and confirmed using PCR genotyping primers listed in Table S1. Col-0 wildtype and the higher-order mutant seeds were surface sterilized and plated on 1X Linsmaier & Skoog (LS) medium (LSP03, Caisson Labs, Smithfield, UT, USA) containing 0.7% (w/v) plant agar (A111, PhytoTech Labs, Lenexa, KS, USA). Seeds were cold stratified for 3 days at 4°C and grown on plates for 2 to 4 weeks, then transferred to soil and grown under the “long-day” condition (16 h light at 23°C / 8 h dark at 18°C). *Agrobacterium tumefaciens* strain GV3101 was used to produce the transgenic plants (in *Atsdr4l-5 dig2* background) expressing *AtSDR4Lpro::3XHA-AtSDR4L-3XFLAG* or *DIG2pro::3XHA-DIG2-3XFLAG* through the floral dip method (Clough and Bent, 1998). Selection of the transgenic lines was carried out on 1X LS medium containing 25 µg/mL Hygromycin B (H-270-1, GoldBio, USA). Seeds were collected from the yellow-to-brown siliques of T2 transgenic plants and dry stored for 12 days, and briefly imbibed for 1 hour at room temperature. Embryos were dissected from the seeds and directly sowed on 1X Linsmaier & Skoog (LS) medium (LSP03, Caisson Labs, Smithfield, UT, USA) with 0.7% (w/v) plant agar for phenotypic observation.

Plasmid construction

The vectors for complementing the *Atsdr4l-5 dig2* mutants were generated as described in the previous study (Lu *et al.*, 2024). Primers listed in TableS1 were used to construct the vector of *AtSDR4Lpro::3xHA-AtSDR4L-3xFLAG* by amplifying the promoter and the fragment containing *3xHA-AtSDR4L-3xFLAG* from an existing plasmid published in the previous study (Lu *et al.*, 2024). *DIG2pro::3xHA-DIG2-3xFLAG* was generated following the similar procedure using primers listed in Table S1. In brief, 2781-bp promoter and the coding sequence (without stop codon) of *DIG2*, N-terminal 3xHA and C-terminal 3xFLAG tags were cloned into the linearized pCAMBIA1300 vector after EcoRI and PstI digests using the NEBuilder® HiFi DNA Assembly Master Mix following the manufacturer’s instructions (E2621S, NEB, Ipswich, MA, USA). Cloning of the vectors pCAMBIA1300-AtSDR4Lpro::3xHA-AtSDR4L-3xFLAG and pCAMBIA1300-DIG2pro::3xHA-DIG2-3xFLAG was performed using *Escherichia coli* competent cells of NEB 10-beta strain (C3019H, NEB, Ipswich, MA, USA) and One Shot™ Mach1™ T1 strain (C862003, Thermo Fisher Scientific, Waltham, MA, USA). The confirmed plasmids were transformed into the *A. tumefaciens* competent cells GV3101 by electroporation.

Germination assays

The physiological characterization of the single and higher-order mutants was carried out using 3 biological replicates for each genotype. Seeds were collected at maturity when siliques turned yellow-to-brown (roughly 18 DAP) and dry stored for 2 weeks. After surface sterilization, seeds were directly sowed, or stratified at 4°C for 3 days and then sowed on 1X LS (LSP03, Caisson Labs, Smithfield, UT, USA) medium with 0.7% (w/v) plant agar, and supplemented with the

following either hormone or hormone antagonists or both: 20 μM gibberellins (GA4 + 7) (G026-1GM, Caisson Labs, Smithfield, UT, USA), 50 μM antabactin (Vaidya *et al.*, 2021), 50 μM ABA-1019 (Diddi *et al.*, 2021), 20 μM GA4 + GA7 with 50 μM antabactin, and 20 μM GA4 + GA7 with 50 μM ABA-1019. DMSO was used as the solvent and included as the mock treatment. Plates were incubated under 16 h light at 23°C / 8 h dark at 17°C, and the ratio of germination was scored for 4 to 7 days after imbibition (DAI). For stress treatments, embryos were isolated from 3-week after-ripened seeds that were cold stratified for 3 days at 4°C. Six embryos were directly sowed on 1X LS medium with 0.7% (w/v) plant agar containing ABA (A-050-1, Gold Biotechnology, St Louis, MO, USA) at 0.1 μM and D-mannitol (A14030, Alfa Aesar, Ward Hill, MA, USA) at 300 mM.

Seed coat bedding assay

Seed coat bedding assay was performed following the protocol by Lee and Lopez-Molina (Lee and Lopez-Molina, 2013). In brief, seeds harvested at maturity (yellow-to-brown siliques, roughly 18 DAP) and dry stored for 2 days were surface sterilized and cold stratified for 3 days at 4°C. Ten to twelve embryos were isolated from the seed coats and sowed directly on the 80-micron nylon mesh or 30 to 40 seed coat beddings on the surface of 1X LSmedium with 0.7% (w/v) plant agar. Plates were incubated under 8 h dark, 17°C / 16 h light, 23°C for 4 days to observe the effect of different bedding strata on seedling establishment.

Periodic acid-propidium iodide (PA-PI) staining

PA-PI staining of Col-0 seedlings and *Atsdr4l-5 dig2* embryos was conducted following procedures described by Truernit et al. and Sliwinska et al. (Truernit *et al.*, 2008; Sliwinska *et al.*, 2009) with minor modifications. After 20 weeks of after-ripening, dissected embryos, transferred on nylon mesh and grown on 1xLS with 0.7 % (w/v) phytoagar medium for two days, were collected and subjected to fixative consisting of 50 % methanol (A412-1, Fisher Scientific, Waltham, MA, USA) and 10 % acetic acid (AA36289AY, Fisher Scientific, Waltham, MA, USA) at 4 C for at least 16 hours. After the wash with water, samples were incubated in 80 % ethanol. Col-0 seedlings were then incubated at 80°C for 8 minutes and *Atsdr4l-5 dig2* embryos were incubated at the same temperature for 3 minutes. Tissues were then rinsed again with water followed by incubation in fixative for 90 minutes. These samples were rewashed with water and then incubated in periodic acid (P7875-2, Sigma-Aldrich, St. Louis, MO, USA) at room temperature for 40 minutes, followed by another round of wash with water. Col-0 seedlings and *Atsdr4l-5 dig2* embryos were then incubated in Schiff reagents with propidium iodide, consisting of 100 mM sodium metabisulphite (P7875-2, Sigma-Aldrich, St. Louis, MO, USA) and 0.15 N HCI with propidium iodide (P1304MP, Invitrogen, Carlsbad, CA, USA) added to a final concentration of 100 ug/mL for 2 hours and 90 minutes, respectively. Col-0 seedlings and *Atsdr4l-5 dig2* embryos underwent the final wash with water hand incubated in a chloral hydrate solution that contains 4 g chloral hydrate (23100, Sigma-Aldrich, St. Louis, MO, USA), 1 mL glycerol (BP2290-1, Fisher Scientific, Waltham, MA, USA), and 2 mL water for 4 days and 16 hours, respectively. Finally, the samples were transferred onto microscope slides and mounted on chloral hydrate for confocal imaging.

Image Acquisition and Processing

Confocal images of PA-PI stained Col-0 seedlings and *Atsdr4l-5 dig2* embryos were obtained using Leica sp5 confocal microscope. Tissues were visualized *via* the excitation wavelength at 514 nm and the emission wavelengths from 570 nm to 620 nm using a 40x objective under Argon laser. Images of the whole embryos from PA-PI staining, and whole seeds and embryos for germination assays and seed-coat bedding assay were acquired using Leica M205 FCA Fluorescence stereo microscope with ColorGainValueR/G/B at 8/1/21 and saturation at 25. PA-PI stained embryos were visualized with objective lens/numerical aperture (NA) at 1x/0.10 and magnification at 2.54. Seedlings used for determining the germination rate were imaged with objective lens/numerical aperture (NA) at 1x/0.02 and magnification at 0.39. Images of the embryos grown on mannitol and ABA media were captured with the objective lens/numerical aperture (NA) at 1x/0.04 and magnification at 0.82. Samples from the seed-coat bedding assay were seen with objective lens/numerical aperture (NA) at 1x/0.03 and magnification at 0.64. Acquired images were processed with Fiji software v1.54k.

Phytohormone measurement

Hormone quantification was performed at the National Research Council Canada, Saskatoon (NRCC SK). Three sets of biological replicates, each containing approximately 55 mg of *Atsdr4l dig2* and 55 mg of Col-0 seeds harvested within two weeks since the siliques turn yellow, were used for hormone profiling. Analysis was performed on a UPLC/ESI-MS/MS utilizing a Waters ACQUITY UPLC system, equipped with a binary solvent delivery manager and a sample manager coupled to a Waters Micromass Quattro Premier XE quadrupole tandem mass spectrometer via a Z-spray interface. MassLynx™ and QuanLynx™ (Micromass, Manchester, UK) were used for data acquisition and data analysis. The procedure for quantitation of ABA, ABA catabolites, auxins, and gibberellins in samples of Arabidopsis seed tissue was performed using a modified procedure described in Lulsdorf et al. (Lulsdorf *et al.*, 2013), while quantitation of ACC was performed using a modified procedure described in Chavaux et al. (Chauvaux *et al.*, 1997). These modifications have not been published. A number of analyte standards namely DPA, ABA-GE, PA, 7'-OH-ABA, neoPA, trans-ABA and IAA-Glu were synthesized and prepared at the National Research Council of Canada, Saskatoon, SK, Canada; ABA, IAA-Leu, IAA-Ala, IAA-Asp, IAA, ACC, phenyl isothiocyanate (PITC), trifluoroacetic acid (TFA) and triethylamine were purchased from Sigma–Aldrich; GAs 1, 3, 4, 7, 8, 9, 19, 20, 24, 29, 44, and 53 were purchased from OlChemim Ltd. (Olomouc, Czech Republic). Deuterated forms of the hormones which were used as internal standards include: d3-DPA, d5-ABA-GE, d3-PA, d4-7'-OH-ABA, d3-neoPA, d4-ABA, d4-trans-ABA, d3-IAA-Leu, d3-IAA-Ala, d3-IAA-Asp, d3-IAA-Glu, and 13C4-IBA were synthesized and prepared at NRCC SK according to Abrams et al. (Abrams *et al.*, 2003) and Zaharia et al. (Zaharia *et al.*, 2005). The d5-IAA was purchased from Cambridge Isotope Laboratories (Andover, MA); 1-amino-[2,2,3,3-d4]-cylopropane-1-carboxylic acid (d4-ACC) was purchased from CDN isotopes (Point-Claire, QC, Canada); d2-GAs 1, 3, 4, 7, 8, 9, 19, 20, 24, 29, 34, 44, 51 and 53 were purchased from OlChemim Ltd. (Olomouc, Czech Republic). The d4-ACC derivative PTH-d4-ACC was used as an internal standard. The deuterated forms of selected hormones used as recovery (external) standards were prepared and synthesized at NRCC SK. Calibration curves were created for all compounds of interest,

including the ACC derivatives, phenylthiohydantoin-ACC (PTH-ACC) and PTH-d4-ACC. Quality control samples (QCs) were run along with the tissue samples.

Seed dissection and RNA extraction

Seeds collected at maturity from yellow-to-brown siliques (roughly 18 DAP) were dry stored for 2 days. Batch dissection of seeds and collection of embryos and seed coat were performed following the procedure described by Iwasaki and Lopez-Molina (Iwasaki and Lopez-Molina, 2021). In brief, seeds were imbibed in water for thirty minutes to two hours at room temperature. Approximately 50 to 100 seeds were gently pressed against two microscope glass slides to break the seed coats. Seed coat (containing endosperm) and intact embryos were manually separated using syringe needles and fine forceps and preserved in RNAlater buffer (AM7020, Thermo Fisher Scientific, Waltham, MA, USA) in a microcentrifuge tube until all samples have been collected. RNAlater buffer was vacated using a syringe before samples were snap frozen in liquid nitrogen. Extraction of total RNA was carried out following the procedure as described in the previous studies (Wu et al., 2022; Lu et al., 2024). Briefly, total RNA was isolated using Spectrum™ Plant Total RNA Kit (STRN50, MilliporeSigma, Burlington, MA, USA), followed by the removal of genomic DNA by DNase I treatment (AM1907, TURBO DNA-free™ Kit, Thermo Fisher Scientific, Waltham, MA, USA).

RNA-seq library preparation

Total RNA from embryo and endosperm-containing seed coat of Col-0 and *Atsdr4l-5 dig2* seeds (same stage and storage conditions as samples for seed coat bedding and seed dissection) were used to make cDNA libraries with three biological replicates each. NEBNext® Ultra II Directional RNA Library Prep Kit for Illumina® (E7760S, NEB, Ipswich, MA, USA) with NEBNext Poly(A) mRNA Magnetic Isolation Module (NEB #E7490) and Unique Dual Index UMI Adaptors RNA Set 1 (E7416S, NEB, Ipswich, MA, USA) were used for library preparation following the manufacturer's instructions. Sequencing was carried out at Novogene with NovaSeq X Plus PE150.

RNA-seq analysis

The public RNA-seq data for mutants of *AtSDR4L* and PRC-related genes were obtained from the following GEO or BioProject accessions: PRJNA663767 for *Atsdr4l-3* and *Atsdr4l-4* (Wu *et al.*, 2022), GSE119715 for *val1 val2* (Yuan *et al.*, 2021), GSE186152 for *pkl* (Liang *et al.*, 2022), GSE186156 for *pkl val1 val2* (Liang *et al.*, 2022), GSE89356 for *bmi1a bmi1b bmi1c* (Zhou *et al.*, 2017), and GSE154697 for *clf28 swn7*, *emf1-2*, and *ring1a ring1b* (Yin *et al.*, 2021). Raw sequencing reads from the public and newly generated tissue-specific RNA-seq data were preprocessed with fastp 0.12.4 for adaptor trimming (Chen *et al.*, 2018), and subsequently aligned to the Arabidopsis TAIR10 reference genome with Araport11 annotation using STAR 2.7.9a and the arguments "--runMode alignReads --outFilterMultimapNmax 10 --outFilterMismatchNoverLmax 0.05 --quantMode GeneCounts --outSAMtype BAM SortedByCoordinate --outReadsUnmapped Fastx" (Dobin *et al.*, 2013). Tiled data files (TDF) were generated from BAM files using igvtools v2.5.3 with the parameters "--includeDuplicates -w 10 -z 5" to specify the maximum zoom level at 5 for precomputing and window size at 10 bp for

averaging coverage (Robinson *et al.*, 2011). TDF files were loaded on Integrative Genomics Viewer 2.14.0 (Robinson *et al.*, 2011) with Araport11 annotations (Cheng *et al.*, 2017) to visualize the transcript abundance at individual loci. Read count data were extracted from the "ReadsPerGene" output file and DEGs were computed using Limma 3.50.3 (Ritchie *et al.*, 2015) in RStudio version 2021.09.2+382 (The R Development Core Team, 2020). Genes were filtered by counts per million (CPM) values greater than 1 in at least 25% of the samples of each study. Library size was normalized using "Trimmed Means of M-values (TMM)" method in edgeR 3.36.0 function "calcNormFactors" (Robinson *et al.*, 2010). Pair-wise correlation among embryo and seed coat samples were computed using $\log_2$(CPM+1) values and graphed by pheatmap 1.0.12 (Kolde, 2019) with viridis colour palettes (Garnier *et al.*, 2021). Log_2 fold changes (LFC) and FDR-adjusted p-values were computed by contrasting the mutants with the wild-type samples. Genes with LFC > and < 0 and adj.P.Val < 0.05 were considered significantly up- and down-regulated. DEGs shared among all the mutants were extracted and intersected using tidyverse 1.3.2 (Wickham *et al.*, 2019). Correlation matrix among the mutants were computed using the LFC values for genes with adj.P.Val < 0.05, and heatmap was created pheatmap 1.0.12 (Kolde, 2019) with viridis colour palettes (Garnier *et al.*, 2021). The LFC values were plotted by ggvenn 0.1.10 for venn diagrams (Yan, 2021), ggplot2 3.5.1 for scatterplots (Wickham, 2009), and pheatmap 1.0.12 using the parameter cutree_rows = 3 for hierarchical clustering (Kolde, 2019), with viridis colour palettes (Garnier *et al.*, 2021). Gene set enrichment analysis (GSEA) of the gene ontology (biological process) terms was performed using the "gseGO" function in clusterProfiler 4.2.2 (Yu *et al.*, 2012) with 100 permutations and org.At.tair.db 3.14.0 annotations (Carlson, 2017). Significantly up-regulated and down-regulated genes in the mutant embryo and seed coat were filtered by LFC > 0.5 and LFC < 0.5, respectively, and ranked by the absolute LFC values by descending order in the corresponding tissues as the input lists for GSEA. Gene-Concept Network plot was generated using the "cnetplot" function in clusterProfiler 4.2.2, using the GSEA results computed by "gseGO" with the uniquely up-regulated DEGs in the embryo (LFC > 0 and adj.P.Val < 0.05 in embryo, and adj.P.Val > 0.05 in seed coat), or uniquely down-regulated DEGs in the seed coat (LFC < 0 and adj.P.Val < 0.05 in seed coat, and adj.P.Val > 0.05 in embryo) as the input (Yu *et al.*, 2012). Differential expression data of ABA-responsive genes were obtained from GSE80565 (Song *et al.*, 2016) for plotting with the DE results from tissue-specific RNA-seq.

Accessions

AtSDR4L and paralogs
AT1G27461 (AtSDR4L/SFL1/ODR1), AT3G48510 (DIG1/SFL2/AITR2), AT5G63350 (DIL1/SFL3/AITR6), AT5G50360 (DIG2/SFL4/AITR5)

Selected epigenetic regulators
AT2G25170 (PKL), AT2G30470 (VAL1), AT4G32010 (VAL2), AT2G30580 (AtBMI1A), AT1G06770 (AtBMI1B), AT3G23060 (AtBMI1C), AT5G44280 (AtRING1A), AT1G03770 (AtRING1B), AT5G11530 (EMF1), AT2G23380 (CLF), AT4G02020 (SWN)

Selected genes in seed-to-seedling transition

AT2G27380 (EPR1), AT3G24650 (ABI3), AT1G18100 (MFT), AT3G24220 (NCED6), AT3G14440 (NCED3), AT4G19230 (CYP707A1), AT2G29090 (CYP707A2), AT5G45340 (CYP707A3), AT4G17870 (PYR1), AT5G53160 (PYL8), AT3G50500 (SNRK2.2), AT4G33950 (SNRK2.6), AT3G26790 (FUS3), AT5G45830 (DOG1), AT4G13260 (YUC2), AT3G44310 (NIT1), AT3G44300 (NIT2), AT1G08980 (AMI1), AT1G02400 (GA2OX6), AT3G03450 (RGL2), AT5G17490 (RGL3), AT2G40610 (EXP8), AT1G28360 (ERF12), AT1G15750 (TPL), AT1G01480 (ACS2), AT5G57390 (AIL5/PLT5/CHO1), AT5G17430 (AIL2/BBM), AT5G13790 (AGL15), AT5G63470 (NF-YC4), AT1G21970 (LEC1), AT1G28300 (LEC2), AT2G36270 (ABI5), AT2G40220 (ABI4), AT2G27230 (LHW)

Acknowledgement

The authors thank Sean Cutler (UCR) and Sue Abrams (USask) for the ABA analogues and discussion. Hormone measurement was carried out by the National Research Council Canada. The model in Fig. 8 was prepared using BioRender.

Author contributions

L.S., B.L. and D.G. conceived and designed the experiments. B.L., D.G., and J.S. performed the experiments. B.L., D.G., and L.S. analyzed the data. B.L., D.G., and L.S.wrote the manuscript.

Funding

The authors thank funding support from the University of British Columbia Four Year Doctoral Fellowships to B.L. and D.G., UBC Work Learn International Undergraduate Research Awards to J.S., and NSERC RGPIN-2019-05039 and CFI JELF/BCKDF 38187 to L.S.

Figures

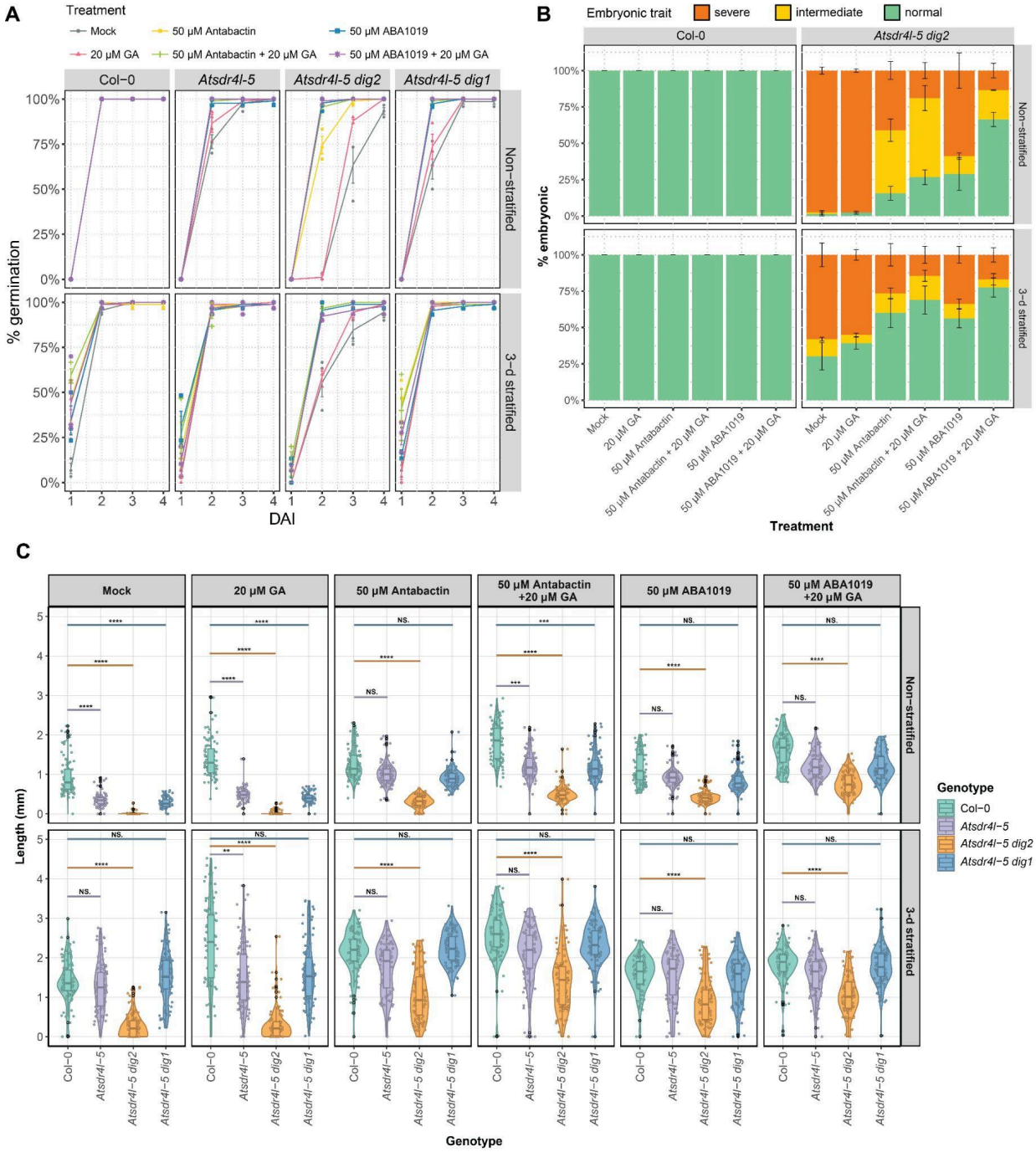

Figure 1. *Atsdr4l-5 dig2* phenotypes are attenuated by ABA antagonists.
A. Germination rate over days after imbibition (DAI) of non-stratified and 3-day cold stratified Col-0, *Atsdr4l-5*, *Atsdr4l-5 dig2* and *Atsdr4l-5 dig1* seeds on 1X LS 0.7 % (w/v) phytoagar medium with treatments of mock, 20 μM GA, 50 μM Antabactin, 50 μM Antabactin + 20 μM GA, 50 μM ABA1019, 50 μM ABA1019 + 20 μM GA. Error bars represent mean ± SEM (24 ≤ n ≤ 30,

3 biological replicates). **B.** Distribution of embryonic traits by severity of Col-0 and *Atsdr4l-5 dig2* seedlings without and with 3-day cold stratification on 1X LS 0.7 % (w/v) phytoagar medium with treatments of mock, 20 μM GA, 50 μM Antabactin, 50 μM Antabactin + 20 μM GA, 50 μM ABA1019, 50 μM ABA1019 + 20 μM GA at 4 DAI. Severe: no root, swollen, opaque hypocotyl; intermediate: short root, opaque hypocotyl; normal: no embryonic trait, resembles wild-type. Error bars represent mean ± SEM. **C.** Embryonic axis quantification of non-stratified and 3-day cold stratified Col-0, *Atsdr4l-5*, *Atsdr4l-5 dig2* and *Atsdr4l-5 dig1* seeds and seedlings at 2 DAI on 1X LS 0.7 % (w/v) phytoagar medium. The black dots represent outliers. $^{**}P < 0.01$, $^{***}P < 0.001$, $^{****}P < 0.0001$ ($24 \leq n \leq 30$, 3 biological replicates, Kruskal-Wallis test, Dunn's test).

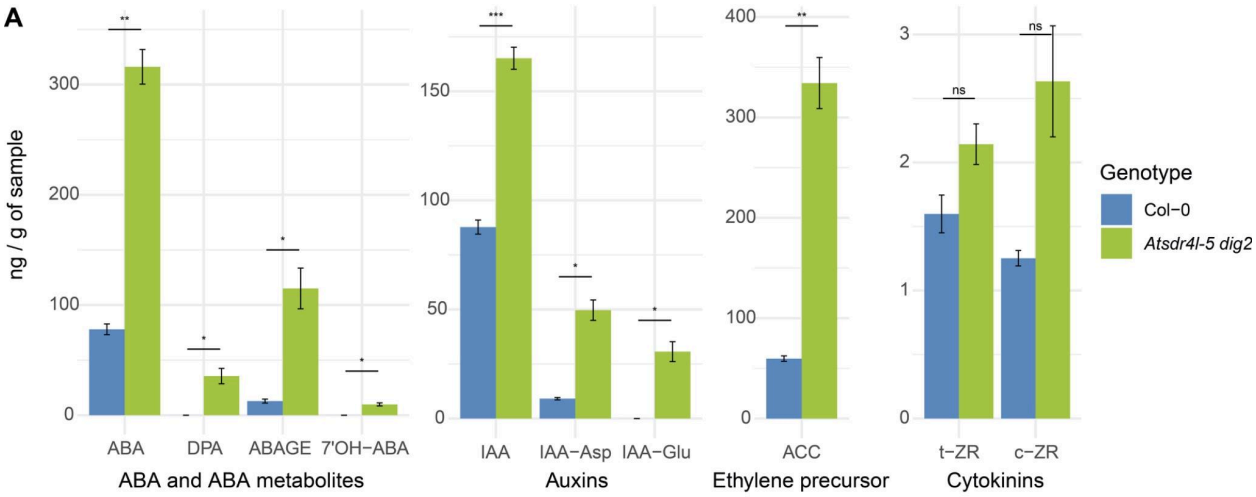

B

			ABA and ABA metabolites (ng/g sample)				Auxins (ng/g sample)			ACC	Cytokinins (ng/g sample)	
Genotype	**replicate**	**weight (mg)**	**ABA**	**DPA**	**ABAGE**	**7'OH-ABA**	**IAA**	**IAA-Asp**	**IAA-Glu**	**(ng/g sample)**	**t-ZR**	**c-ZR**
Col-0	1	55	87		13		83	8		65	2	1
Col-0	2	59	71		10		86	9		58	1	1
Col-0	3	49	75		16		94	10		57	2	1
		Average	**77.938**		**12.789**		**87.743**	**9.102**		**59.744**	**1.598**	**1.252**
		SEM	4.856		1.766		3.223	0.535		2.682	0.147	0.060
Atsdr4l-5 dig2	1	55	296.161	22.303	78.600	10.969	175.198	54.845	36.929	378.793	2.049	2.884
Atsdr4l-5 dig2	2	48	347.181	38.249	138.697	11.385	160.817	40.344	33.264	333.056	2.452	3.227
Atsdr4l-5 dig2	3	56	305.011	45.976	127.707	7.055	159.423	53.807	21.786	290.714	1.927	1.789
		Average	**316.118**	**35.510**	**115.001**	**9.803**	**165.146**	**49.665**	**30.659**	**334.188**	**2.143**	**2.634**
		SEM	15.741	6.970	18.475	1.379	5.042	4.670	4.561	25.433	0.159	0.434

Figure 2. Multiple phytohormones are mis-regulated in mature *Atsdr4l-5 dig2* seeds.
A. Bar plots for the quantification (ng / g of sample) of ABA and ABA metabolites, auxin and its derivatives, ethylene precursor and cytokinins in seeds. Error bars represent mean ± SEM. *$P < 0.05$, **$P < 0.01$, ***$P < 0.001$ (3 biological replicates, two-tailed Student's t-test). **B.** Summary table for the amounts of hormones and metabolites detected in Col-0 and *Atsdr4l-5 dig2* seeds.

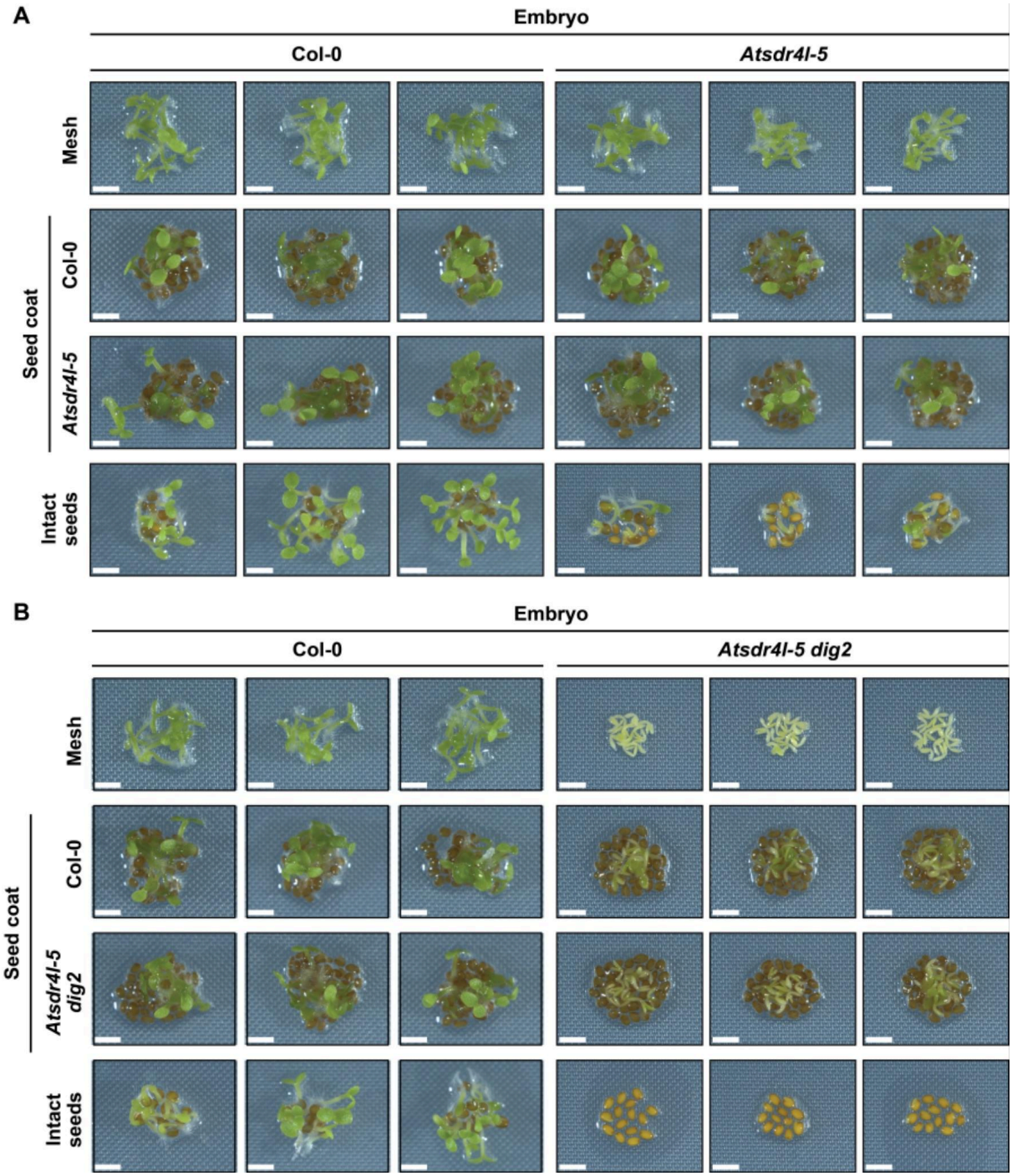

Figure 3. Dormancy in *Atsdr4l-5 dig2* is contributed by both the embryo and the seed coat. **A-B.** Establishment of Col-0 and *Atsdr4l-5* (A) or *Atsdr4l-5 dig2* (B) embryos directly on the medium (with mesh), and the seed coats of Col-0 and the corresponding mutant, and intact seeds at 3 DAI on 1XLS 0.7 % (w/v) phytoagar medium. Each column represents one set of biological replicates. Scale bar = 2 mm.

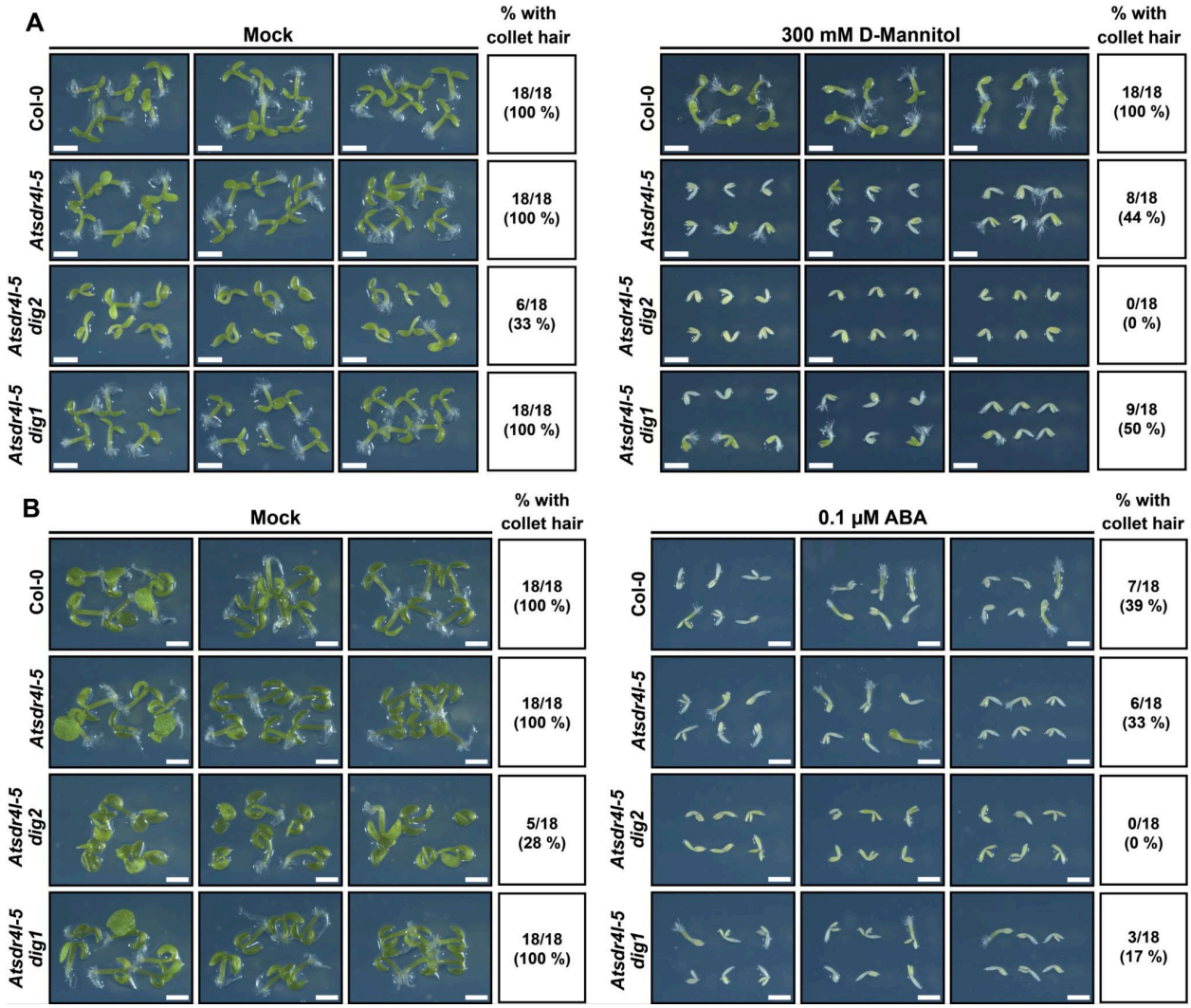

Figure 4. *Atsdr4l-5 dig2* embryo has hypersensitivity to osmotic stress and ABA.
A. Embryos at 3 DAI on mock- (left) and 300 mM D-Mannitol- (right) treated 1X LS 0.7 % (w/v) phytoagar medium. **B.** Embryos at 7 DAI on mock- (left) and 0.1 μM ABA- (right) treated 1X LS 0.7 % phytoagar (w/v) medium. Each column represents one set of biological replicates. Scale bar = 2 mm.

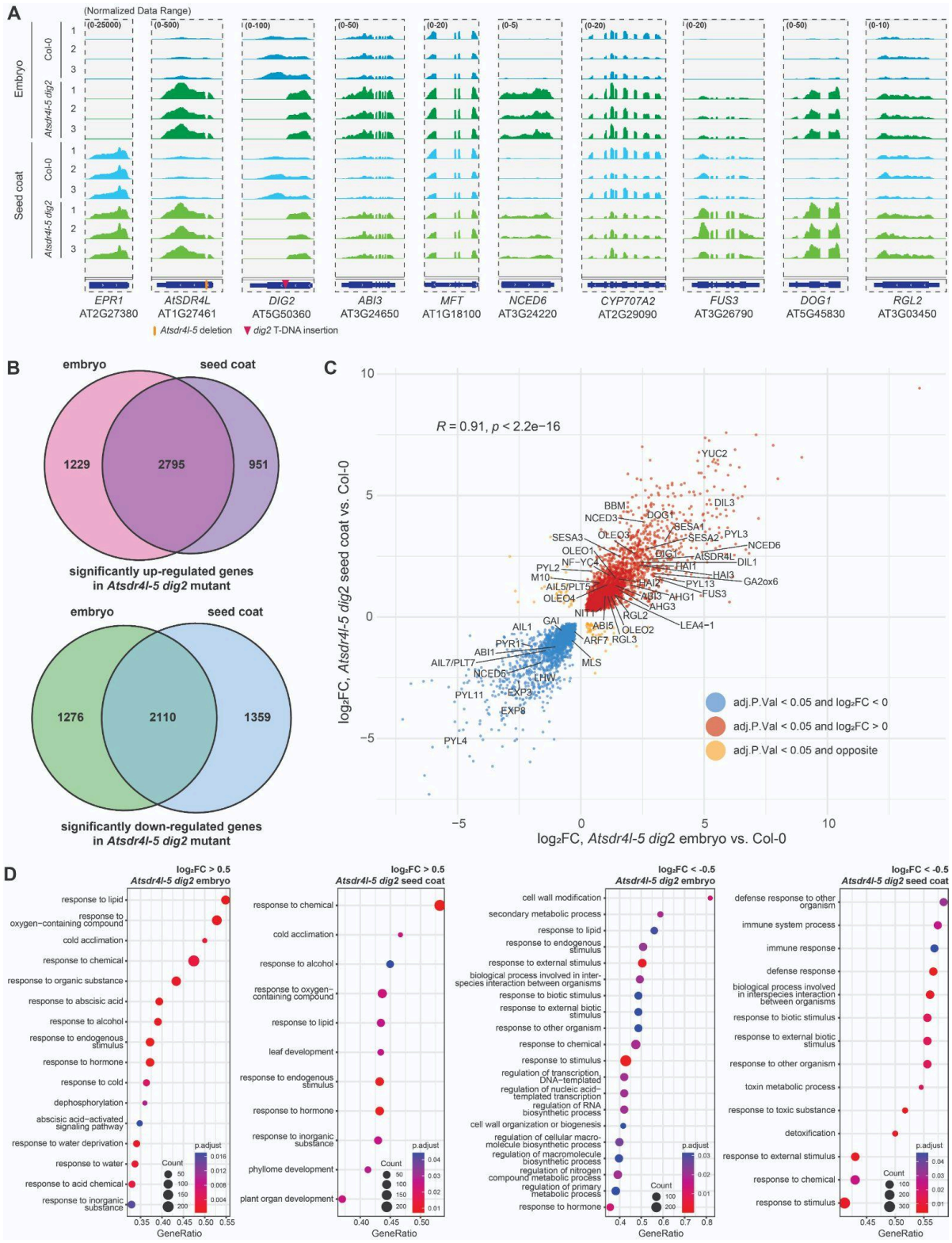

Figure 5. *Atsdr4l-5 dig2* embryo and seed coat show both similar and unique misregulation of genes.

A. Integrative Genomics Viewer (IGV) showing the differential expression (DE) of *AtSDR4L*, *DIG2*, and selected marker genes in seed dormancy and ABA regulation in Col-0 and *Atsdr4l-5 dig2* embryo and seed coat. Diamond-shape and triangle labels mark the position of segmental deletion and T-DNA insertion at *AtSDR4L* and *DIG2* loci. Numbers in parentheses specify the range of normalized data in tiled data format. **B.** Venn diagram for the overlaps of significantly up-regulated (adj.P.Val < 0.05, $\log_2$FC > 0) and down-regulated (adj.P.Val < 0.05, $\log_2$FC < 0) genes between the mutant embryo and seed coat. **C.** Scatterplot showing the correlation in the magnitudes of misregulation ($\log_2$FC computed against Col-0) for significantly DE genes in the *Atsdr4l-5 dig2* mutant embryo and seed coat. Colour of the dots are labelled for the directions of misregulation. Selected genes involved in regulating embryogenesis, seed dormancy, storage reserve accumulation, ABA and GA metabolism and signaling, and auxin-related pathways are annotated. **D.** Dot plots with the results of gene set enrichment analysis (GSEA) for Gene Ontology (GO) terms (biological process) associated with significantly up-regulated (adj.P.Val < 0.05, $\log_2$FC > 0.5) and down-regulated (adj.P.Val < 0.05, $\log_2$FC < -0.5) genes in *Atsdr4l-5 dig2* embryo and seed coat. The size of the dots is proportional to the number of genes with the corresponding GO annotation, and the colour represents the scale of adjusted p-values.

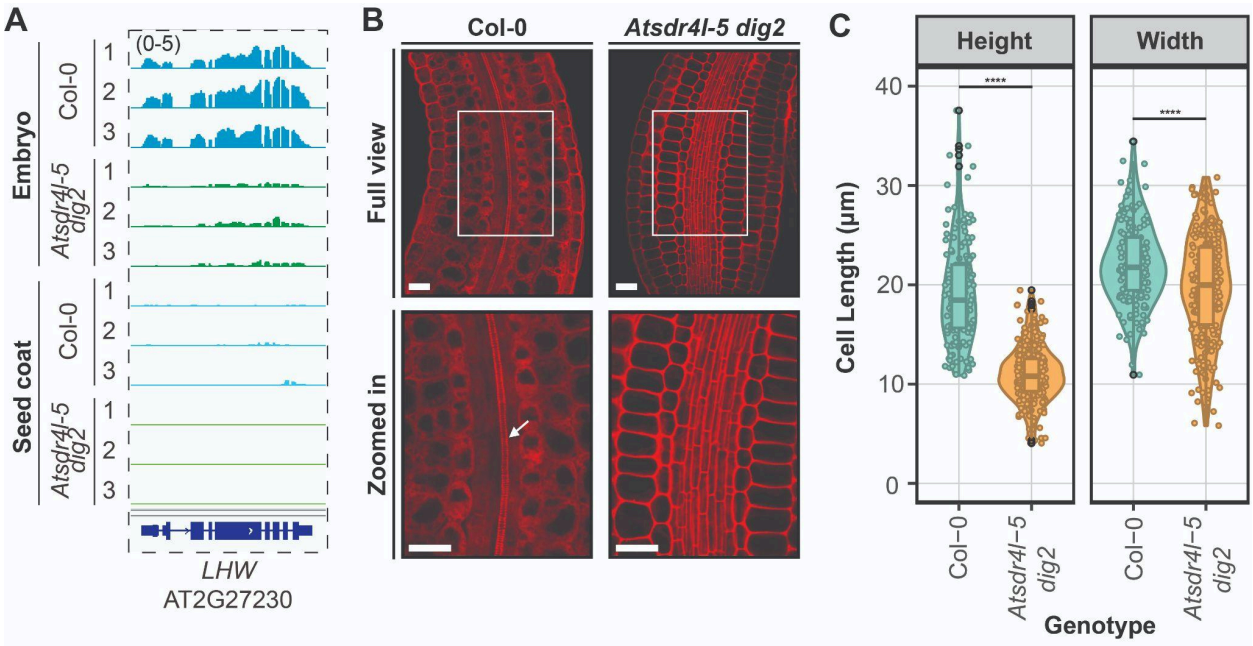

Figure 6. *Atsdr4l-5 dig2* embryo exhibits delayed cell differentiation and elongation. .
A. Integrative Genomics Viewer (IGV) screenshots for *LONESOME HIGHWAY* (*LHW*) involved in protoxylem differentiation, with strong reduction of expression in *Atsdr4l-5 dig2* embryo. Numbers in parentheses indicate the range of normalized data in tiled data format. **B.** Confocal image of periodic acid - propidium iodide (PA-PI)-stained embryos grown on 1X LS 0.7 % (w/v) phytoagar medium for 2 days. Arrow in the enlarged view of the Col-0 sample indicates protoxylem. Scale bar = 25 µm. **C.** Height and width of cells at the cortex of embryos. ****$P < 0.0001$ ($48 \leq n \leq 89$, 3 biological replicates, Two-Tailed Student's t-Test).

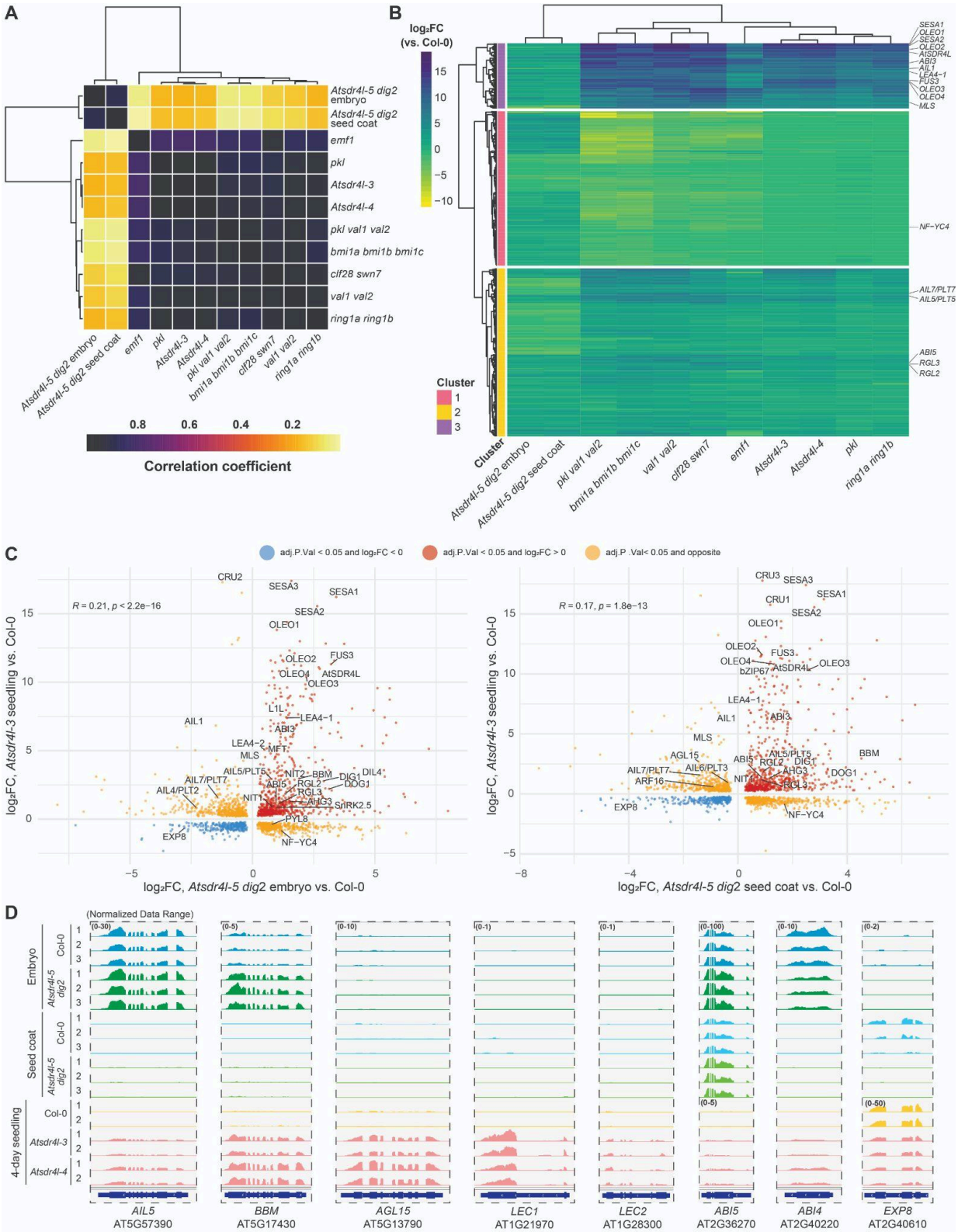

Figure 7. Transcriptome changes in *Atsdr4l-5 dig2* seeds lay the groundwork for altered developmental paths in seedlings.

A. Heatmap for the pairwise correlation within the transcriptomes of *Atsdr4l-5 dig2* mutant embryo and seed coat, and *Atsdr4l* and *prc* mutant seedlings. Correlation matrix was computed using $\log_2$FC of all shared genes among the mutants filtered by adj.P.Val < 0.05. Colour scale represents the correlation coefficients. **B.** Heatmap showing the differential expression in $\log_2$FC (mutant vs. Col-0) of all shared significantly dysregulated genes (adj.P.Val < 0.05) among *Atsdr4l-5 dig2*, *Atsdr4l* and *prc* mutants. Columns representing sample genotypes and rows corresponding to genes are organized by hierarchical clustering, with labels for genes of interest related to embryogenesis, seed dormancy, storage reserve accumulation, ABA and GA metabolism and signaling, and auxin-related pathways. Colour scale reflects the $\log_2$FC values. **C.** Scatterplot showing the distribution of $\log_2$FC values for significantly (adj.P.Val < 0.05) DE genes between *Atsdr4l-5 dig2* mutant embryo and *Atsdr4l-3* mutant seedling at 4 DAI (left), and between *Atsdr4l-5 dig2* mutant seed coat and *Atsdr4l-3* mutant seedling (right). Dots are color-coded for the directions of misregulation. Genes involved in seed maturation and hormone pathways of interest are highlighted. **D.** Integrative Genomics Viewer (IGV) screenshots for representative genes involved in regulating embryogenesis and/or dormancy-germination switch, with similar or opposite DE trends between *Atsdr4l-5 dig2* seed compartments and *Atsdr4l* mutant seedlings. Numbers in parentheses indicate the range of normalized data in tiled data format.

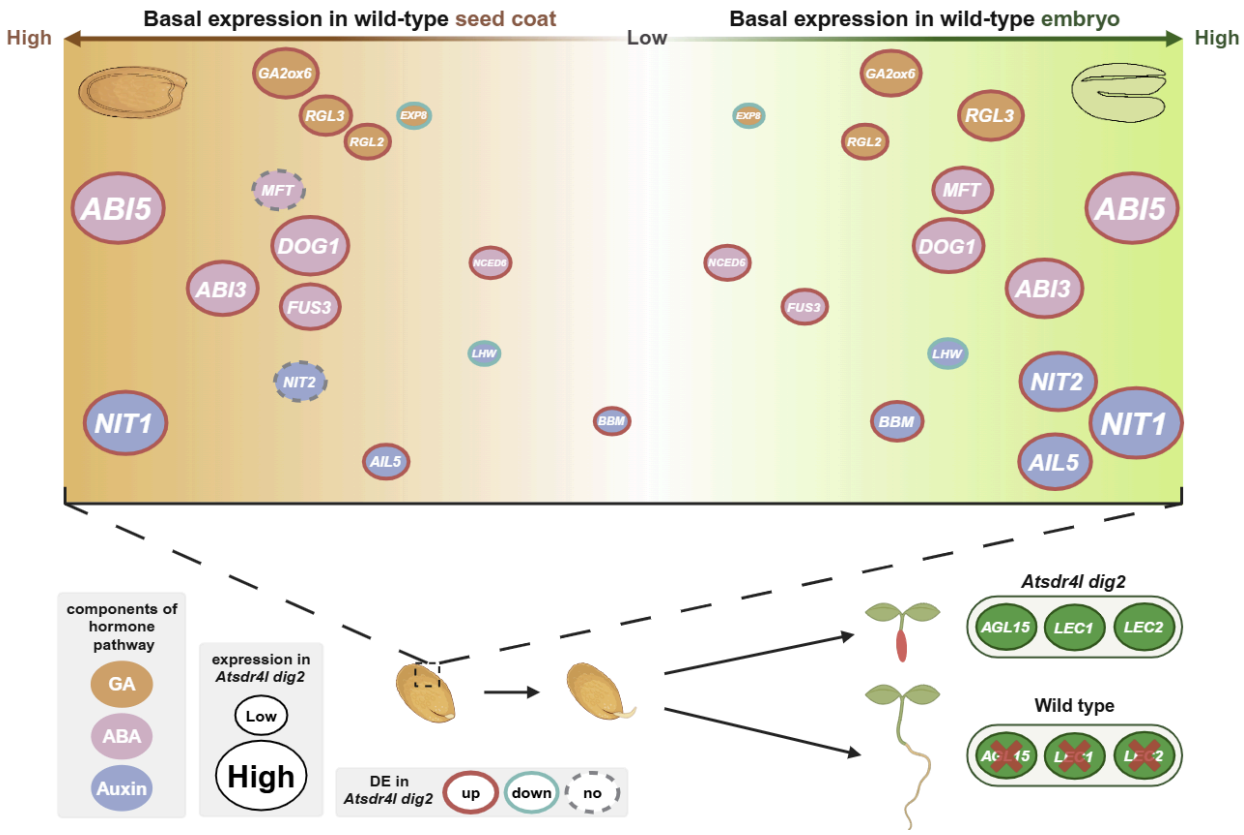

Figure 8. Proposed model for the tissue-specific regulation by AtSDR4L and DIG2 on selected dormancy and development genes in the embryo and seed coat.
In mature wild-type seeds, AtSDR4L works synergistically with DIG2 to repress the positive regulators of ABA and auxin biosynthesis and signaling, as well as the negative regulators in the GA signaling to promote the release of dormancy and subsequent seedling establishment. The basal level of gene expression in the wild-type seed compartments, approximated by $\log_2$(FPKM), is indicated by the position of the gene along the horizontal axis. The size of the ellipses reflects transcript abundance of indicated genes in *Atsdr4l-5 dig2*, and ellipse outline indicates whether the gene is differentially expressed. Many of these genes exhibit preferential expression in either the seed coat or the embryo. Ellipse color reflects whether the gene is involved in biosynthesis, signaling, or downstream responses of indicated hormones. Genes related to multiple hormones are assigned to one. Positive regulators of embryogenesis *LEC1*, *LEC2*, and *AGL15* are not mis-regulated in *Atsdr4l-5 dig2* mutant seeds, but are up-regulated in *Atsdr4l* seedlings that exhibit embryonic traits (Wu *et al.*, 2022).

SI Figures

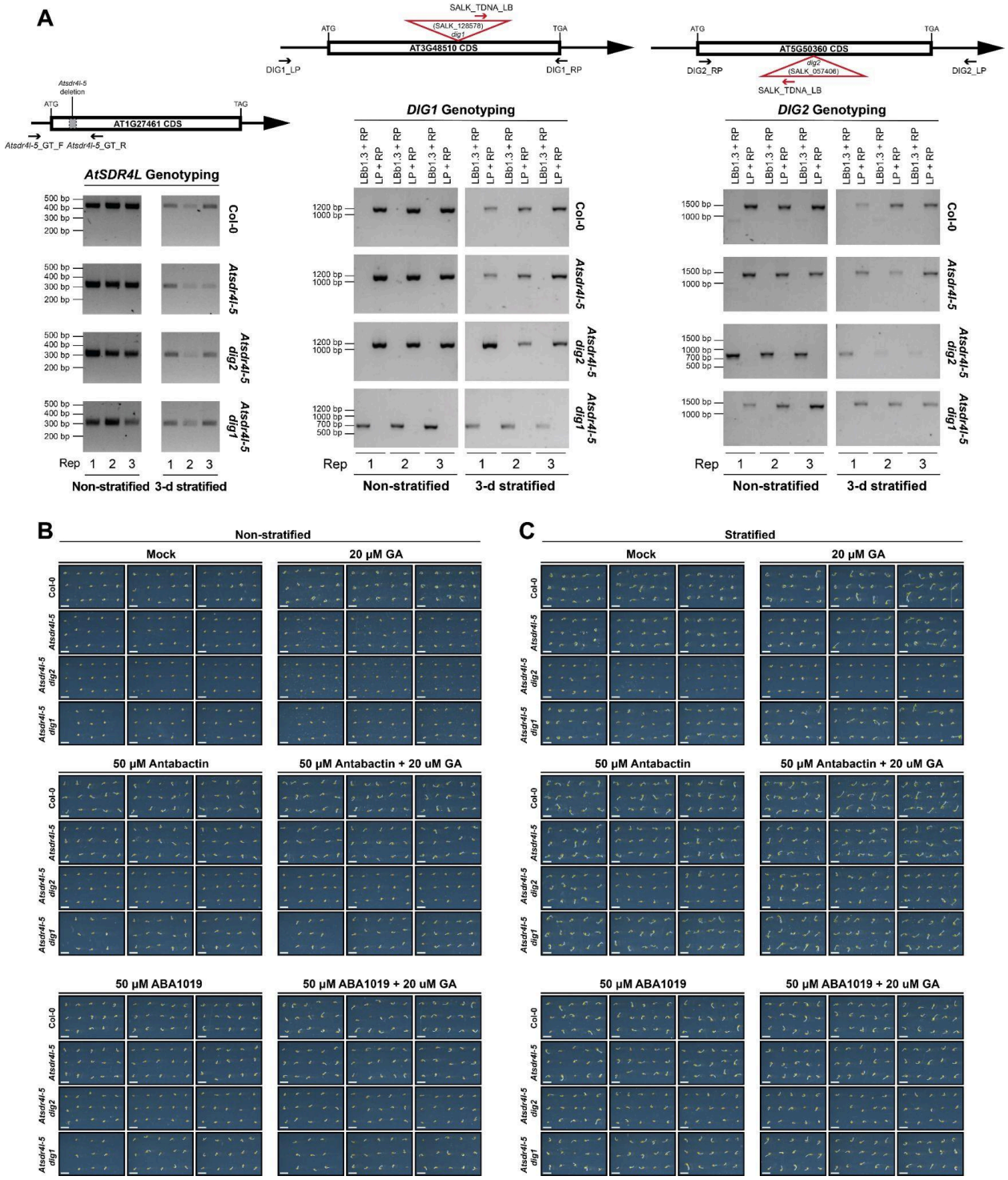

Figure S1. Growth defects of *Atsdr4l-5 dig2* are alleviated by ABA antagonists.
A. A diagram of CRISPR/Cas9-mediated deletion that is harboured in *Atsdr4l-5* allele and T-DNA insertion map of *dig1* (SALK_128578) and *dig2* (SALK_057406) (top). Genotyping of

Col-0, *Atsdr4l-5*, *Atsdr4l-5 dig2*, *Atsdr4l-5 dig1* used in this study (bottom). **B.** Germination and embryonic axis length of non-stratified (left) and 3-day-stratified (right) Col-0, *Atsdr4l-5*, *Atsdr4l-5 dig2*, *Atsdr4l-5 dig1* seeds and seedlings at 2 days after imbibition (2 DAI) post 2 weeks of dry storage on 1xLS 0.7 % (w/v) phytoagar medium with treatments of 20 μM GA, 50 μM Antabactin, 50 μM Antabactin + 20 μM GA, 50 μM ABA1019, 50 μM ABA1019 + 20 μM GA-treated 1xLS 0.7 % (w/v) phytoagar medium. Each column represents one set of biological replicates. Scale bar = 4 mm.

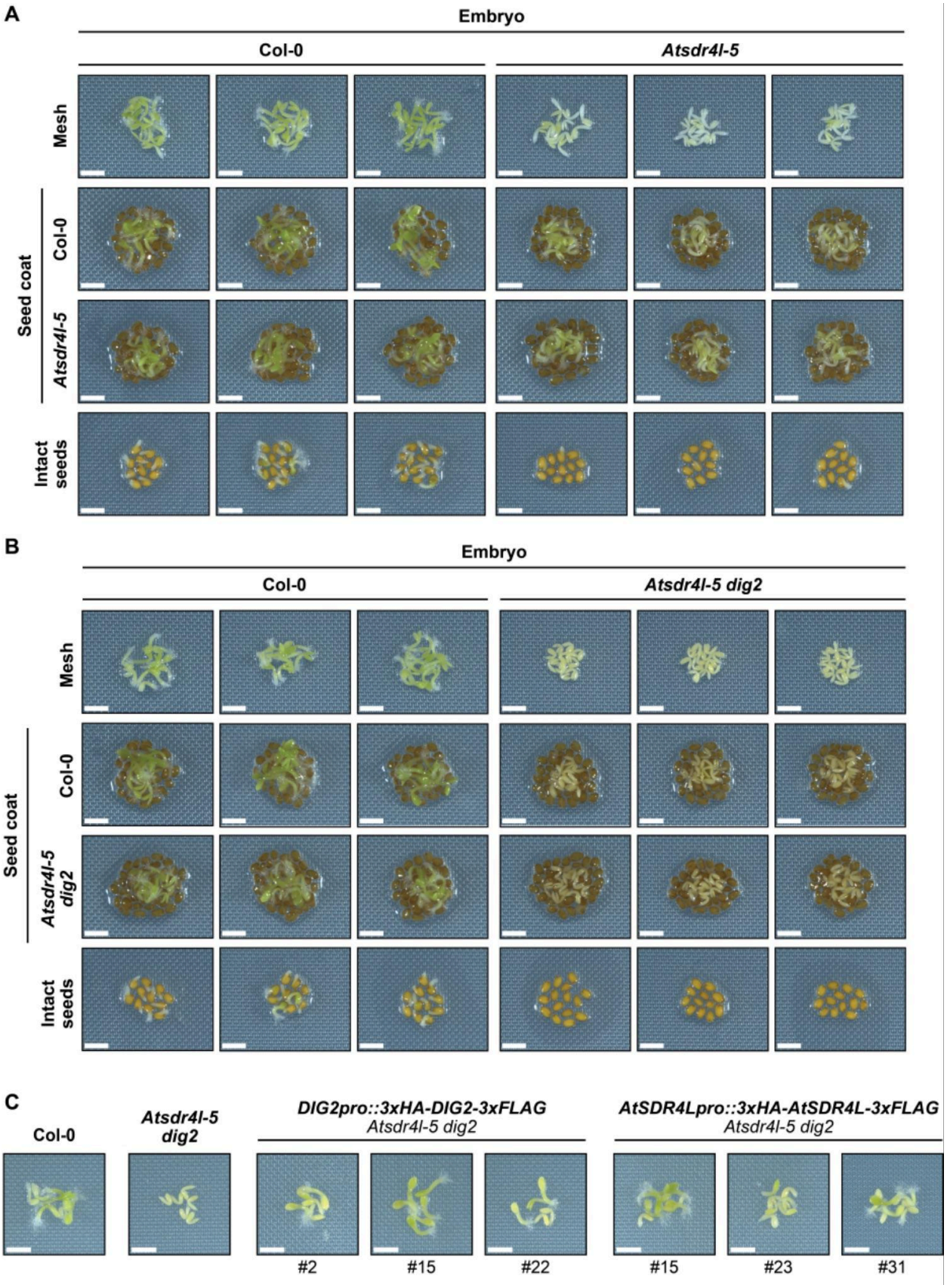
A
Embryo
Col-0
Atsdr4l-5
Mesh
Seed coat
Col-0
Atsdr4l-5
Intact seeds
B
Embryo
Col-0
Atsdr4l-5 dig2
Mesh
Seed coat
Col-0
Atsdr4l-5 dig2
Intact seeds
C
Col-0
Atsdr4l-5 dig2
DIG2pro::3xHA-DIG2-3xFLAG
Atsdr4l-5 dig2
AtSDR4Lpro::3xHA-AtSDR4L-3xFLAG
Atsdr4l-5 dig2
#2
#15
#22
#15
#23
#31

Figure S2. Dormancy and growth inhibition of *Atsdr4l-5 dig2* are exerted by the embryo and the seed coat

A-B. Establishment of Col-0 and *Atsdr4l-5* (A) or *Atsdr4l-5 dig2* (B) embryos directly on the medium (with mesh), and the seed coats of Col-0 and the corresponding mutant, and intact seeds at 2 DAI on 1XLS 0.7 % (w/v) phytoagar medium. Each column represents one set of biological replicates. Scale bar = 2 mm. **C.** Complementation of *Atsdr4l-5 dig2* mutant embryos from non-stratified T2 seeds by the vectors of *DIG2pro::3xHA-DIG2-3XFLAG* or *AtSDR4Lpro::3xHA-AtSDR4L-3XFLAG*. Embryos were imaged at 3 DAI. Scale bar = 2 mm.

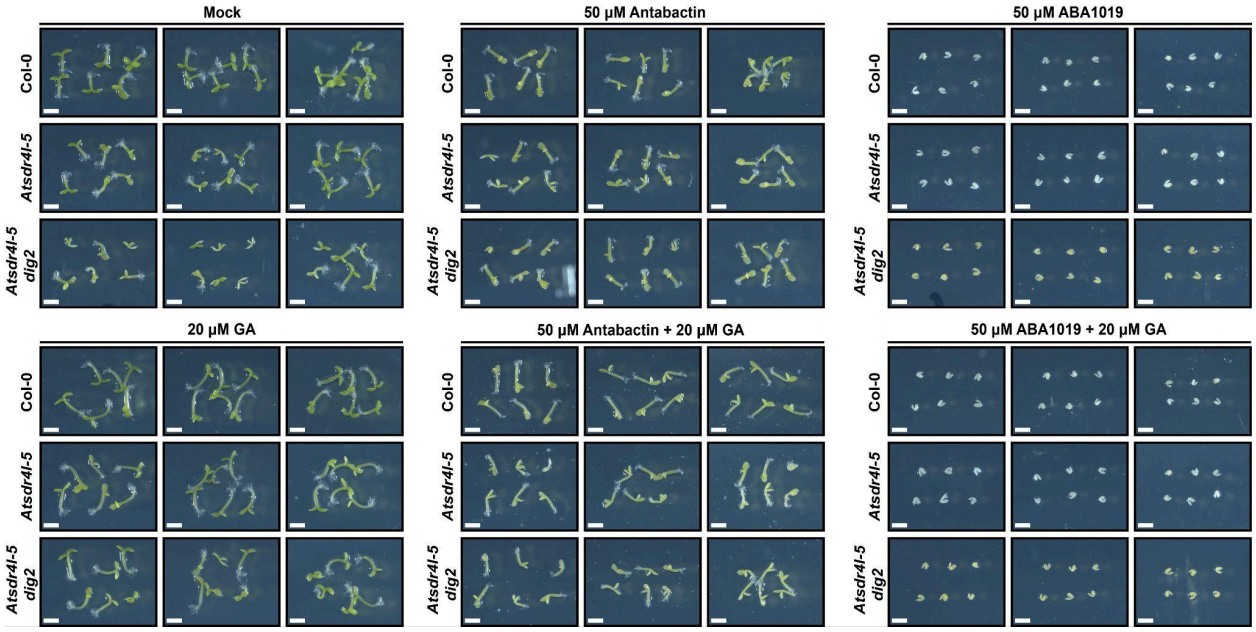

Figure S3. Wild-type and *Atsdr4l-5 dig2* embryos exhibit ABA analogue-specific responses in seedling establishment

Embryos at 3 DAI on 1X LS 0.7 % (w/v) phytoagar medium with treatments of mock, 20 μM GA, 50 μM Antabactin, 50 μM Antabactin + 20 μM GA, 50 μM ABA1019, 50 μM ABA1019 + 20 μM GA after 2 weeks of dry storage. Each column represents one set of biological replicates. Scale bar = 2 mm.

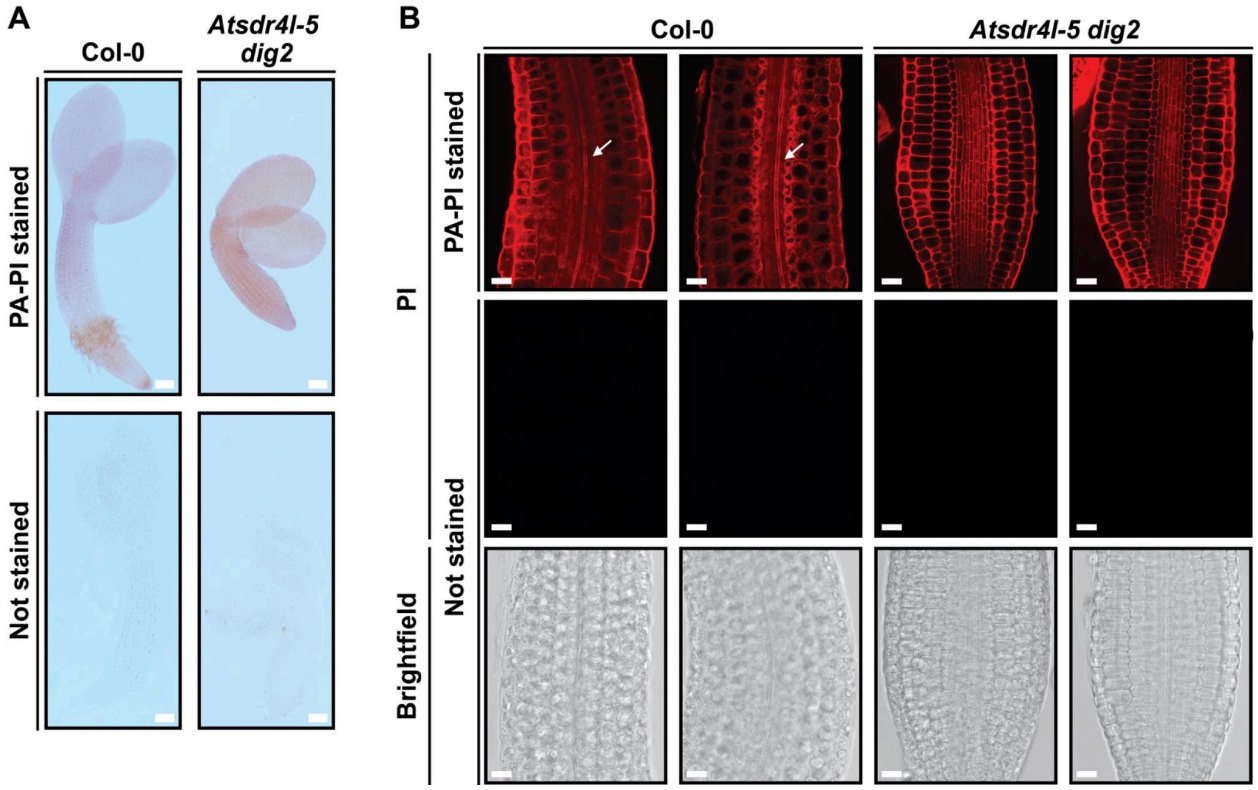

Figure S4. *Atsdr4l-5 dig2* embryo exhibits delayed cell elongation and differentiation
A. Representative images from periodic acid - propidium iodide (PA-PI)-stained embryos grown on 1xLS 0.7 % (w/v) phytoagar medium for 2 days. Col-0 and *Atsdr4l-5 dig2* seeds were dry-stored for 20 weeks and cold-stratified for three days before dissection. Scale bar = 0.15 mm. **B.** Confocal images of embryos with (top row) or without (middle and bottom rows) PA-PI staining. Arrows in the Col-0 samples indicate protoxylem. Scale bar = 25 µm.

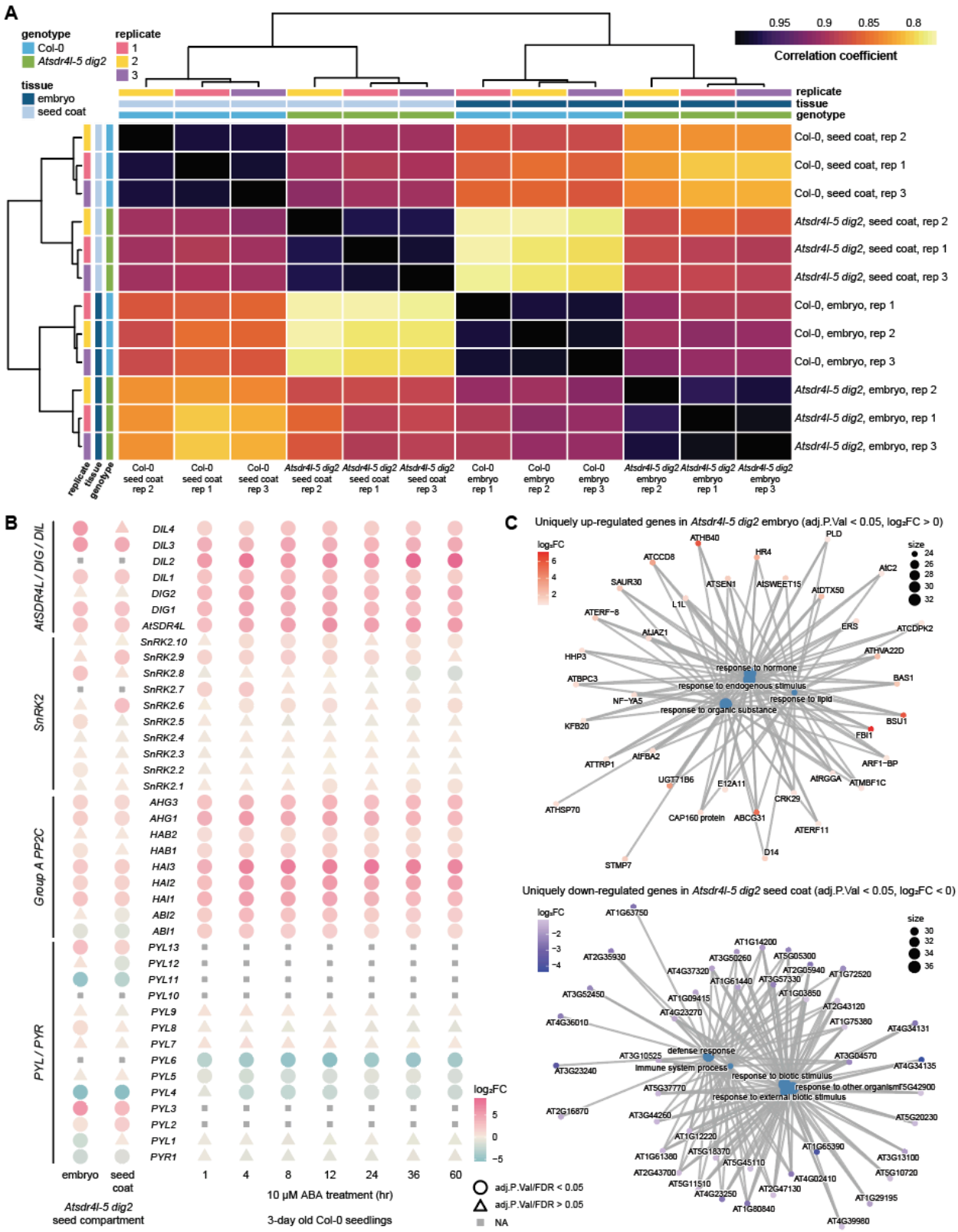
A
genotype
Col-0
Atsdr4l-5 dig2
replicate
1
2
3
tissue
embryo
seed coat
0.95 0.9 0.85 0.8
Correlation coefficient
replicate
tissue
genotype
Col-0, seed coat, rep 2
Col-0, seed coat, rep 1
Col-0, seed coat, rep 3
Atsdr4l-5 dig2, seed coat, rep 2
Atsdr4l-5 dig2, seed coat, rep 1
Atsdr4l-5 dig2, seed coat, rep 3
Col-0, embryo, rep 1
Col-0, embryo, rep 2
Col-0, embryo, rep 3
Atsdr4l-5 dig2, embryo, rep 2
Atsdr4l-5 dig2, embryo, rep 1
Atsdr4l-5 dig2, embryo, rep 3
Col-0 seed coat rep 2
Col-0 seed coat rep 1
Col-0 seed coat rep 3
Atsdr4l-5 dig2 seed coat rep 2
Atsdr4l-5 dig2 seed coat rep 1
Atsdr4l-5 dig2 seed coat rep 3
Col-0 embryo rep 1
Col-0 embryo rep 2
Col-0 embryo rep 3
Atsdr4l-5 dig2 embryo rep 2
Atsdr4l-5 dig2 embryo rep 1
Atsdr4l-5 dig2 embryo rep 3
B
AtSDR4L / DIG / DIL
DIL4
DIL3
DIL2
DIL1
DIG2
DIG1
AtSDR4L
SnRK2
SnRK2.10
SnRK2.9
SnRK2.8
SnRK2.7
SnRK2.6
SnRK2.5
SnRK2.4
SnRK2.3
SnRK2.2
SnRK2.1
Group A PP2C
AHG3
AHG1
HAB2
HAB1
HAI3
HAI2
HAI1
ABI2
ABI1
PYL / PYR
PYL13
PYL12
PYL11
PYL10
PYL9
PYL8
PYL7
PYL6
PYL5
PYL4
PYL3
PYL2
PYL1
PYR1
embryo
seed coat
Atsdr4l-5 dig2 seed compartment
1 4 8 12 24 36 60
10 µM ABA treatment (hr)
3-day old Col-0 seedlings
log2FC
5
0
−5
adj.P.Val/FDR < 0.05
adj.P.Val/FDR > 0.05
NA
C
Uniquely up-regulated genes in Atsdr4l-5 dig2 embryo (adj.P.Val < 0.05, log2FC > 0)
log2FC
6
4
2
size
24
26
28
30
32
ATHB40
PLD
HR4
ATCCD8
AIC2
SAUR30
ATSEN1
AtSWEET15
AtDTX50
L1L
ATERF-8
ERS
ATCDPK2
AUAZ1
ATHVA22D
HHP3
response to hormone
ATBPC3
response to endogenous stimulus
BAS1
NF-YA5
response to lipid
response to organic substance
KFB20
BSU1
FBI1
AtFBA2
ATTRP1
ARF1-BP
UGT71B6
E12A11
AtRGGA
ATMBF1C
CRK29
ATHSP70
CAP160 protein
ABCG31
ATERF11
D14
STMP7
Uniquely down-regulated genes in Atsdr4l-5 dig2 seed coat (adj.P.Val < 0.05, log2FC < 0)
log2FC
−2
−3
−4
size
30
32
34
36
AT1G63750
AT1G14200
AT2G35930
AT3G50260
AT5G05300
AT4G37320
AT2G05940
AT1G72520
AT1G61440
AT3G57330
AT3G52450
AT1G09415
AT1G03850
AT4G23270
AT2G43120
AT4G36010
AT1G75380
AT4G34131
AT3G10525
defense response
AT3G04570
AT3G23240
immune system process
AT4G34135
response to biotic stimulus
AT5G37770
response to other organism
AT5G42900
response to external biotic stimulus
AT2G16870
AT3G44260
AT5G20230
AT1G12220
AT1G65390
AT1G61380
AT5G18370
AT3G13100
AT5G45110
AT2G43700
AT5G10720
AT4G02410
AT5G11510
AT2G47130
AT4G23250
AT1G29195
AT1G80840
AT4G39980

Figure S5. *Atsdr4l-5 dig2* transcriptome changes correlate with tissues and exhibit compartment-specific differential gene expression.

A. Heatmap for the pairwise correlation among the Col-0 and *Atsdr4l-5 dig2* embryo and seed coat samples. Correlation matrix was computed using $\log_2$ transformed (with pseudo-count of 1) counts per million (CPM) values after filtering out genes with low read counts and normalizing library size by "Trimmed Means of M-values (TMM)" method. Colour scale represents the correlation coefficients. **B.** Dotted heat scale reflecting the up-regulation or down-regulation of genes encoding components of ABA signaling pathways in *Atsdr4l-5 dig2* embryo and seed coat, as well as in ABA-treated Col-0 seedlings (data from GSE80565). *PYR*/*PYL*: *PYRABACTIN RESISTANCE1*/*PYR1-LIKE* ABA receptors; *PP2C*: protein phosphatase 2C; *SnRK2*: *SNF1-RELATED PROTEIN KINASE2*; *AtS*DR4L/DIG/DIL: *ARABIDOPSIS THALIANA SEED DORMANCY 4-LIKE*/*Dynamic Influencer of Gene Expression*/*DIG-Like*. Shapes indicate whether the differential expression is significant in the corresponding tissue or treatment. Genes without detectable expression are indicated by NA. **C.** Gene-Concept Network plots showing the linkage of enriched GO terms (biological process) with genes uniquely up-regulated (adj.P.Val < 0.05, $\log_2$FC > 0) only in *Atsdr4l-5 dig2* embryo, and uniquely down-regulated in *Atsdr4l-5 dig2* seed coat. GSEA did not reveal significantly enriched GO terms using uniquely down-regulated genes in embryo or uniquely up-regulated genes in endosperm. The size of dots corresponds to the number of genes associated with each functional category, and colour scale indicates the magnitude of up-regulation in *Atsdr4l-5 dig2* embryo compared to Col-0 in $\log_2$FC values.

SI Tables

Supplementary Table 1: Primers

Genotyping and qPCR primers

Primer name	Primer sequence (5’ - 3’)
*Atsdr4l-5*_GT_F	ACCTTCCCTACCTCATCAC
*Atsdr4l-5*_GT_R	ACTAGAAGAACCGCATGACG
SALK_TDNA_LBb1.3	ATTTTGCCGATTTCGGAAC
Salkseq057406.2_DIG2_LP	TGCATTCCATTGTGTGATTAAAC
Salkseq057406.2_DIG2_RP	TATTGCGAGGTACGGTGGTAG
Salkseq128578.0_DIG1_LP	ACTCCAACACGTGTCCAGATC
Salkseq128578.0_DIG1_RP	TGATCTAACGGTGTCAAAGGC

Cloning primers - Complementation constructs for Arabidopsis transformation

Construct	Primer name	Primer sequence (5’ - 3’)
pCAMBIA1300-AtSDR4Lpro-3xHA-AtSDR4L-3xFLAG	HiFi_pCAMBIA1300_EcoRI_SDR4pro_F	CAGCTATGACCATGATTAC GAATTC CAGAGGATGAATCGGCC
	HiFi_SDR4pro_SpeI_3xHA_R	TGGCTAGAACTAGTGACGTCAAGAATGATAAAAAAAAAAAACTC
	HiFi_SDR4pro_SpeI_3xHA_F	TCTTGACGTCACTAGTTCTAGCCATGTACCCGTA
	HiFi_pCAMBIA1300_PstI_3xFLAG_R	GATGATACGAACGAAAGCT CTGCAG TCACTTATCGTCATCGTCCTTG
pCAMBIA1300-DIG2pro-3xHA-DIG2-3xFLAG	HiFi_pCAMBIA1300_EcoRI_DIG2pro_F	CAGCTATGACCATGATTACGAATTC aattggtagagcaggaatcc
	HiFi_DIG2pro_3xHA_R	catacgggtacatggctaga GTTTTGTCTAACAAACAAGTTTGTTTTGTT
	HiFi_DIG2pro_3xHA_F	ACTTGTTTGTTAGACAAAAC tctagccatgtacccgtatg
	3xHA_DIG2_R	CCCGGAAATT tcctgcgtagtctgggacgt
	3xHA_DIG2_F	ctacgcagga AATTTCCGGGGAGGTTGTTG

	DIG2_3xFLAG_R	cttcgaaccagggccctggcgc CCGTCCAAGGCAAAGTGCAG
	DIG2_3xFLAG_F	CGG gcGCCAGGGCCCTGGTTCGAAGACTACAAA
	HiFi_pCAMBIA1300_PstI_3xFLAG_R	GATGATACGAACGAAAGCT CTGCAG TCACTTATCGTCATCGTCCTTG

References

Abrams SR, Nelson K, Ambrose SJ. 2003. Deuterated abscisic acid analogs for mass spectrometry and metabolism studies. Journal of Labelled Compounds and Radiopharmaceuticals **46**, 273–283.

Ahammed GJ, Gantait S, Mitra M, Yang Y, Li X. 2020. Role of ethylene crosstalk in seed germination and early seedling development: A review. Plant Physiology and Biochemistry **151**, 124–131.

Alizadeh M, Hoy R, Lu B, Song L. 2021. Team effort: Combinatorial control of seed maturation by transcription factors. Current Opinion in Plant Biology **63**, 102091.

Bai Y-L, Yin X, Xiong C-F, Cai B-D, Wu Y, Zhang X-Y, Wei Z, Ye T, Feng Y-Q. 2022. Neophaseic acid catabolism in the 9′-hydroxylation pathway of abscisic acid in Arabidopsis thaliana. Plant Communications **3**, 100340.

Baskin JM, Baskin CC. 2004. A classification system for seed dormancy. Seed Science Research **14**, 1–16.

Baskin CC, Baskin JM. 2020. Breaking Seed Dormancy during Dry Storage: A Useful Tool or Major Problem for Successful Restoration via Direct Seeding? Plants **9**, 636.

Bassel GW, Stamm P, Mosca G, Barbier De Reuille P, Gibbs DJ, Winter R, Janka A, Holdsworth MJ, Smith RS. 2014. Mechanical constraints imposed by 3D cellular geometry and arrangement modulate growth patterns in the *Arabidopsis* embryo. Proceedings of the National Academy of Sciences **111**, 8685–8690.

Beaudoin N, Serizet C, Gosti F, Giraudat J. 2000. Interactions between Abscisic Acid and Ethylene Signaling Cascades. The Plant Cell **12**, 1103–1115.

Belin C, Megies C, Hauserová E, Lopez-Molina L. 2009. Abscisic Acid Represses Growth of the Arabidopsis Embryonic Axis after Germination by Enhancing Auxin Signaling. The Plant Cell **21**, 2253–2268.

Bethke PC, Libourel IGL, Aoyama N, Chung Y-Y, Still DW, Jones RL. 2007. The Arabidopsis Aleurone Layer Responds to Nitric Oxide, Gibberellin, and Abscisic Acid and Is Sufficient and Necessary for Seed Dormancy. Plant Physiology **143**, 1173–1188.

Boutilier K, Offringa R, Sharma VK, *et al.* 2002. Ectopic Expression of BABY BOOM Triggers a Conversion from Vegetative to Embryonic Growth. The Plant Cell **14**, 1737–1749.

Cao H, Han Y, Li J, Ding M, Li Y, Li X, Chen F, Soppe WJ, Liu Y. 2020. Arabidopsis thaliana SEED DORMANCY 4-LIKE regulates dormancy and germination by mediating the gibberellin pathway. (G Leubner, Ed.). Journal of Experimental Botany **71**, 919–933.

Carlson M. 2017. org.At.tair.db.

Carrillo-Barral N, Rodríguez-Gacio M del C, Matilla AJ. 2020. Delay of Germination-1 (DOG1): A Key to Understanding Seed Dormancy. Plants **9**, 480.

Chauvaux N, Van Dongen W, Esmans EL, Van Onckelen HA. 1997. Quantitative analysis of 1-aminocyclopropane-1-carboxylic acid by liquid chromatography coupled to electrospray tandem mass spectrometry. Journal of Chromatography A **775**, 143–150.

Chen B, Fiers M, Dekkers BJW, Maas L, Van Esse GW, Angenent GC, Zhao Y, Boutilier K. 2021. ABA signalling promotes cell totipotency in the shoot apex of germinating embryos. (A Murphy, Ed.). Journal of Experimental Botany **72**, 6418–6436.

Chen B, Maas L, Figueiredo D, *et al.* 2022. BABY BOOM regulates early embryo and endosperm development. Proceedings of the National Academy of Sciences **119**, e2201761119.

Chen S, Zhou Y, Chen Y, Gu J. 2018. fastp: an ultra-fast all-in-one FASTQ preprocessor. Bioinformatics **34**, i884–i890.

Cheng C, Krishnakumar V, Chan AP, Thibaud-Nissen F, Schobel S, Town CD. 2017. Araport11: a complete reannotation of the *Arabidopsis thaliana* reference genome. The Plant

Journal **89**, 789–804.
Clough SJ, Bent AF. 1998. Floral dip: a simplified method forAgrobacterium-mediated transformation ofArabidopsis thaliana: Floral dip transformation of Arabidopsis. The Plant Journal **16**, 735–743.
Debeaujon I, Léon-Kloosterziel KM, Koornneef M. 2000. Influence of the Testa on Seed Dormancy, Germination, and Longevity in Arabidopsis. Plant Physiology **122**, 403–414.
Dekkers BJW, He H, Hanson J, Willems LAJ, Jamar DCL, Cueff G, Rajjou L, Hilhorst HWM, Bentsink L. 2016. The Arabidopsis *DELAY OF GERMINATION 1* gene affects *ABSCISIC ACID INSENSITIVE 5 (ABI5)* expression and genetically interacts with *ABI3* during Arabidopsis seed development. The Plant Journal **85**, 451–465.
Diddi N, Lai L, Brookbank BP, *et al.* 2021. 3′-(Phenyl alkynyl) analogs of abscisic acid: synthesis and biological activity of potent ABA antagonists. Organic & Biomolecular Chemistry **19**, 2978–2985.
Dobin A, Davis CA, Schlesinger F, Drenkow J, Zaleski C, Jha S, Batut P, Chaisson M, Gingeras TR. 2013. STAR: ultrafast universal RNA-seq aligner. Bioinformatics **29**, 15–21.
Dubreucq B, Berger N, Vincent E, Boisson M, Pelletier G, Caboche M, Lepiniec L. 2000. The *Arabidopsis AtEPR1* extensin‐like gene is specifically expressed in endosperm during seed germination. The Plant Journal **23**, 643–652.
Finch‐Savage WE, Leubner‐Metzger G. 2006. Seed dormancy and the control of germination. New Phytologist **171**, 501–523.
Frey A, Effroy D, Lefebvre V, Seo M, Perreau F, Berger A, Sechet J, To A, North HM, Marion-Poll A. 2012. Epoxycarotenoid cleavage by NCED5 fine-tunes ABA accumulation and affects seed dormancy and drought tolerance with other NCED family members: Functional analysis of the NCED5 gene. The Plant Journal **70**, 501–512.
Gajdošová S, Spíchal L, Kamínek M, *et al.* 2011. Distribution, biological activities, metabolism, and the conceivable function of cis-zeatin-type cytokinins in plants. Journal of Experimental Botany **62**, 2827–2840.
Garnier S, Ross N, BoB Rudis, Filipovic-Pierucci A, Galili T, Timelyportfolio, Greenwell B, Sievert C, Harris DJ, JJ Chen. 2021. sjmgarnier/viridis: viridis 0.6.0 (pre-CRAN release).
Gazzarrini S, Song L. 2024. LAFL Factors in Seed Development and Phase Transitions. Annual Review of Plant Biology doi: 10.1146/annurev-arplant-070623-111458.
Gazzarrini S, Tsai AY-L. 2015. Hormone cross-talk during seed germination. (T Guilfoyle and G Hagen, Eds.). Essays in Biochemistry **58**, 151–164.
Ghassemian M, Nambara E, Cutler S, Kawaide H, Kamiya Y, McCourt P. 2000. Regulation of Abscisic Acid Signaling by the Ethylene Response Pathway in Arabidopsis. The Plant Cell **12**, 1117–1126.
Go D, Lu B, Alizadeh M, Gazzarrini S, Song L. 2024. Voice from both sides: a molecular dialogue between transcriptional activators and repressors in seed-to-seedling transition and crop adaptation. Frontiers in Plant Science **15**, 1416216.
Gonzalez-Guzman M, Pizzio GA, Antoni R, *et al.* 2012. *Arabidopsis* PYR/PYL/RCAR Receptors Play a Major Role in Quantitative Regulation of Stomatal Aperture and Transcriptional Response to Abscisic Acid. The Plant Cell **24**, 2483–2496.
Graeber K, Linkies A, Steinbrecher T, *et al.* 2014. *DELAY OF GERMINATION 1* mediates a conserved coat-dormancy mechanism for the temperature- and gibberellin-dependent control of seed germination. Proceedings of the National Academy of Sciences **111**.
Horstman A, Li M, Heidmann I, Weemen M, Chen B, Muino JM, Angenent GC, Boutilier K. 2017. The BABY BOOM Transcription Factor Activates the LEC1-ABI3-FUS3-LEC2 Network to Induce Somatic Embryogenesis. Plant Physiology **175**, 848–857.
Horstman A, Willemsen V, Boutilier K, Heidstra R. 2014. AINTEGUMENTA-LIKE proteins: hubs in a plethora of networks. Trends in Plant Science **19**, 146–157.
Iwasaki M, Lopez-Molina L. 2021. Arabidopsis thaliana Mature Endosperm Dissection and

Isolation of Genomic DNA from Mature Seed Tissues. In: Cho J, ed. Methods in Molecular Biology. Plant Transposable Elements. New York, NY: Springer US, 239–243.
Iwasaki M, Penfield S, Lopez-Molina L. 2022. Parental and Environmental Control of Seed Dormancy in *Arabidopsis thaliana*. Annual Review of Plant Biology **73**, 355–378.
Kang J, Yim S, Choi H, Kim A, Lee KP, Lopez-Molina L, Martinoia E, Lee Y. 2015. Abscisic acid transporters cooperate to control seed germination. Nature Communications **6**, 8113.
Kolde R. 2019. pheatmap: Pretty Heatmaps.
Kucera B, Cohn MA, Leubner-Metzger G. 2005. Plant hormone interactions during seed dormancy release and germination. Seed Science Research **15**, 281–307.
Kushiro T, Okamoto M, Nakabayashi K, Yamagishi K, Kitamura S, Asami T, Hirai N, Koshiba T, Kamiya Y, Nambara E. 2004. The Arabidopsis cytochrome P450 CYP707A encodes ABA 8′-hydroxylases: key enzymes in ABA catabolism. The EMBO Journal **23**, 1647–1656.
Lee KP, Lopez-Molina L. 2013. A Seed Coat Bedding Assay to Genetically Explore In Vitro How the Endosperm Controls Seed Germination in Arabidopsis thaliana. Journal of Visualized Experiments, 50732.
Lee KP, Piskurewicz U, Tureckova V, Strnad M, Lopez-Molina L. 2010. A seed coat bedding assay shows that RGL2-dependent release of abscisic acid by the endosperm controls embryo growth in Arabidopsis dormant seeds. Proceedings of the National Academy of Sciences **107**, 19108–19113.
Lefebvre V, North H, Frey A, Sotta B, Seo M, Okamoto M, Nambara E, Marion-Poll A. 2006. Functional analysis of Arabidopsis *NCED6* and *NCED9* genes indicates that ABA synthesized in the endosperm is involved in the induction of seed dormancy. The Plant Journal **45**, 309–319.
Li X, Chen T, Li Y, Wang Z, Cao H, Chen F, Li Y, Soppe WJJ, Li W, Liu Y. 2019. ETR1/RDO3 Regulates Seed Dormancy by Relieving the Inhibitory Effect of the ERF12-TPL Complex on *DELAY OF GERMINATION1* Expression. The Plant Cell **31**, 832–847.
Liang Z, Yuan L, Xiong X, *et al.* 2022. The transcriptional repressors VAL1 and VAL2 mediate genome-wide recruitment of the CHD3 chromatin remodeler PICKLE in Arabidopsis. The Plant Cell, koac217.
Liu X, Hu P, Huang M, Tang Y, Li Y, Li L, Hou X. 2016. The NF-YC–RGL2 module integrates GA and ABA signalling to regulate seed germination in Arabidopsis. Nature Communications **7**, 12768.
Liu F, Zhang H, Ding L, Soppe WJJ, Xiang Y. 2020. REVERSAL OF RDO5 1, a Homolog of Rice Seed Dormancy4, Interacts with bHLH57 and Controls ABA Biosynthesis and Seed Dormancy in Arabidopsis. The Plant Cell **32**, 1933–1948.
Lu B, Alizadeh M, Hoy R, Zheng R, Go D, Song L. 2024. Co-repressors AtSDR4L and DIG1 interact with transcription factor VAL2 and promote Arabidopsis seed-to-seedling transition. Plant Physiology, kiae225.
Lulsdorf MM, Yuan HY, Slater SMH, Vandenberg A, Han X, Zaharia LI, Abrams SR. 2013. Endogenous hormone profiles during early seed development of C. arietinum and C. anatolicum. Plant Growth Regulation **71**, 191–198.
Mano Y, Nemoto K. 2012. The pathway of auxin biosynthesis in plants. Journal of Experimental Botany **63**, 2853–2872.
Nakabayashi K, Bartsch M, Xiang Y, Miatton E, Pellengahr S, Yano R, Seo M, Soppe WJJ. 2012. The Time Required for Dormancy Release in *Arabidopsis* Is Determined by DELAY OF GERMINATION1 Protein Levels in Freshly Harvested Seeds. The Plant Cell **24**, 2826–2838.
Nakashima K, Fujita Y, Kanamori N, *et al.* 2009. Three Arabidopsis SnRK2 Protein Kinases, SRK2D/SnRK2.2, SRK2E/SnRK2.6/OST1 and SRK2I/SnRK2.3, Involved in ABA Signaling are Essential for the Control of Seed Development and Dormancy. Plant and Cell Physiology **50**, 1345–1363.
Nambara E, Marion-Poll A. 2005. ABSCISIC ACID BIOSYNTHESIS AND CATABOLISM.

Annual Review of Plant Biology **56**, 165–185.
Nambara E, Okamoto M, Tatematsu K, Yano R, Seo M, Kamiya Y. 2010. Abscisic acid and the control of seed dormancy and germination. Seed Science Research **20**, 55–67.
Ogas J, Cheng J-C, Sung ZR, Somerville C. 1997. Cellular Differentiation Regulated by Gibberellin in the *Arabidopsis thaliana pickle* Mutant. Science **277**, 91–94.
Ohashi-Ito K, Bergmann DC. 2007. Regulation of the *Arabidopsis* root vascular initial population by *LONESOME HIGHWAY*. Development **134**, 2959–2968.
Ohashi-Ito K, Matsukawa M, Fukuda H. 2013. An Atypical bHLH Transcription Factor Regulates Early Xylem Development Downstream of Auxin. Plant and Cell Physiology **54**, 398–405.
Okamoto M, Kuwahara A, Seo M, Kushiro T, Asami T, Hirai N, Kamiya Y, Koshiba T, Nambara E. 2006. CYP707A1 and CYP707A2, Which Encode Abscisic Acid 8′-Hydroxylases, Are Indispensable for Proper Control of Seed Dormancy and Germination in Arabidopsis. Plant Physiology **141**, 97–107.
Penfield S. 2017. Seed dormancy and germination. Current Biology **27**, R874–R878.
Peterson FC, Burgie ES, Park S-Y, Jensen DR, Weiner JJ, Bingman CA, Chang C-EA, Cutler SR, Phillips GN, Volkman BF. 2010. Structural basis for selective activation of ABA receptors. Nature Structural & Molecular Biology **17**, 1109–1113.
Piskurewicz U, Jikumaru Y, Kinoshita N, Nambara E, Kamiya Y, Lopez-Molina L. 2008. The Gibberellic Acid Signaling Repressor RGL2 Inhibits *Arabidopsis* Seed Germination by Stimulating Abscisic Acid Synthesis and ABI5 Activity. The Plant Cell **20**, 2729–2745.
Ritchie ME, Phipson B, Wu D, Hu Y, Law CW, Shi W, Smyth GK. 2015. limma powers differential expression analyses for RNA-sequencing and microarray studies. Nucleic Acids Research **43**, e47–e47.
Robinson MD, McCarthy DJ, Smyth GK. 2010. edgeR : a Bioconductor package for differential expression analysis of digital gene expression data. Bioinformatics **26**, 139–140.
Robinson JT, Thorvaldsdóttir H, Winckler W, Guttman M, Lander ES, Getz G, Mesirov JP. 2011. Integrative genomics viewer. Nature Biotechnology **29**, 24–26.
Sajeev N, Koornneef M, Bentsink L. 2024. A commitment for *life:* Decades of unraveling the molecular mechanisms behind seed dormancy and germination. The Plant Cell **36**, 1358–1376.
Samalova M, Melnikava A, Elsayad K, *et al.* 2023. Hormone-regulated expansins: Expression, localization, and cell wall biomechanics in Arabidopsis root growth. Plant Physiology **194**, 209–228.
Schäfer M, Brütting C, Meza-Canales ID, Großkinsky DK, Vankova R, Baldwin IT, Meldau S. 2015. The role of *cis* -zeatin-type cytokinins in plant growth regulation and mediating responses to environmental interactions. Journal of Experimental Botany **66**, 4873–4884.
Skubacz A, Daszkowska-Golec A. 2017. Seed Dormancy: The Complex Process Regulated by Abscisic Acid, Gibberellins, and Other Phytohormones that Makes Seed Germination Work. In: El-Esawi M, ed. Phytohormones - Signaling Mechanisms and Crosstalk in Plant Development and Stress Responses. InTech.
Sliwinska E, Bassel GW, Bewley JD. 2009. Germination of Arabidopsis thaliana seeds is not completed as a result of elongation of the radicle but of the adjacent transition zone and lower hypocotyl. Journal of Experimental Botany **60**, 3587–3594.
Song L, Huang S -s. C, Wise A, Castanon R, Nery JR, Chen H, Watanabe M, Thomas J, Bar-Joseph Z, Ecker JR. 2016. A transcription factor hierarchy defines an environmental stress response network. Science **354**, aag1550–aag1550.
Stamm P, Ravindran P, Mohanty B, Tan EL, Yu H, Kumar PP. 2012. Insights into the molecular mechanism of RGL2-mediated inhibition of seed germination in Arabidopsis thaliana. BMC Plant Biology **12**, 179.
Tan B-C, Joseph LM, Deng W-T, Liu L, Li Q-B, Cline K, McCarty DR. 2003. Molecular characterization of the *Arabidopsis* 9 *-cis* epoxycarotenoid dioxygenase gene family: AtNCED

gene family in Arabidopsis. The Plant Journal **35**, 44–56.
The R Development Core Team. 2020. R: A Language and Environment for Statistical Computing.
Truernit E, Bauby H, Dubreucq B, Grandjean O, Runions J, Barthélémy J, Palauqui J-C. 2008. High-Resolution Whole-Mount Imaging of Three-Dimensional Tissue Organization and Gene Expression Enables the Study of Phloem Development and Structure in *Arabidopsis*. The Plant Cell **20**, 1494–1503.
Tsuchisaka A, Theologis A. 2004. Unique and Overlapping Expression Patterns among the Arabidopsis 1-Amino-Cyclopropane-1-Carboxylate Synthase Gene Family Members. Plant Physiology **136**, 2982–3000.
Tsukagoshi H, Morikami A, Nakamura K. 2007. Two B3 domain transcriptional repressors prevent sugar-inducible expression of seed maturation genes in *Arabidopsis* seedlings. Proceedings of the National Academy of Sciences **104**, 2543–2547.
Tsuwamoto R, Yokoi S, Takahata Y. 2010. Arabidopsis EMBRYOMAKER encoding an AP2 domain transcription factor plays a key role in developmental change from vegetative to embryonic phase. Plant Molecular Biology **73**, 481–492.
Vaidya AS, Peterson FC, Eckhardt J, *et al.* 2021. Click-to-lead design of a picomolar ABA receptor antagonist with potent activity in vivo. Proceedings of the National Academy of Sciences **118**, e2108281118.
Weitbrecht K, Müller K, Leubner-Metzger G. 2011. First off the mark: early seed germination. Journal of Experimental Botany **62**, 3289–3309.
Wickham H. 2009. *ggplot2*. New York, NY: Springer New York.
Wickham H, Averick M, Bryan J, *et al.* 2019. Welcome to the Tidyverse. Journal of Open Source Software **4**, 1686.
Wu T, Alizadeh M, Lu B, *et al.* 2022. The transcriptional co-repressor SEED DORMANCY 4-LIKE (AtSDR4L) promotes the embryonic-to-vegetative transition in *Arabidopsis thaliana*. Journal of Integrative Plant Biology **64**, 2075–2096.
Xi W, Liu C, Hou X, Yu H. 2010. MOTHER OF FT AND TFL1 Regulates Seed Germination through a Negative Feedback Loop Modulating ABA Signaling in Arabidopsis. The Plant Cell **22**, 1733–1748.
Yamagami T, Tsuchisaka A, Yamada K, Haddon WF, Harden LA, Theologis A. 2003. Biochemical Diversity among the 1-Amino-cyclopropane-1-Carboxylate Synthase Isozymes Encoded by the Arabidopsis Gene Family. Journal of Biological Chemistry **278**, 49102–49112.
Yan L. 2021. ggvenn: Draw Venn Diagram by ‘ggplot2’. 0.1.10.
Yang C, Bratzel F, Hohmann N, Koch M, Turck F, Calonje M. 2013. VAL- and AtBMI1-Mediated H2Aub Initiate the Switch from Embryonic to Postgerminative Growth in Arabidopsis. Current Biology **23**, 1324–1329.
Yang SF, Hoffman NE. ETHYLENE BIOSYNTHESIS AND ITS REGULATION IN HIGHER PLANTS. *in press*.
Yang L, Liu S, Lin R. 2020*a*. The role of light in regulating seed dormancy and germination. Journal of Integrative Plant Biology **62**, 1310–1326.
Yang J-F, Yin C-Y, Wang D, Jia C-Y, Hao G-F, Yang G-F. 2020*b*. Molecular Determinants Elucidate the Selectivity in Abscisic Acid Receptor and HAB1 Protein Interactions. Frontiers in Chemistry **8**, 425.
Yano R, Kanno Y, Jikumaru Y, Nakabayashi K, Kamiya Y, Nambara E. 2009. CHOTTO1, a Putative Double APETALA2 Repeat Transcription Factor, Is Involved in Abscisic Acid-Mediated Repression of Gibberellin Biosynthesis during Seed Germination in Arabidopsis. Plant Physiology **151**, 641–654.
Yin X, Romero-Campero FJ, de Los Reyes P, *et al.* 2021. H2AK121ub in Arabidopsis associates with a less accessible chromatin state at transcriptional regulation hotspots. Nature Communications **12**, 315.

Yu G, Wang L-G, Han Y, He Q-Y. 2012. clusterProfiler: an R Package for Comparing Biological Themes Among Gene Clusters. OMICS: A Journal of Integrative Biology **16**, 284–287.
Yuan L, Song X, Zhang L, Yu Y, Liang Z, Lei Y, Ruan J, Tan B, Liu J, Li C. 2021. The transcriptional repressors VAL1 and VAL2 recruit PRC2 for genome-wide Polycomb silencing in *Arabidopsis*. Nucleic Acids Research **49**, 98–113.
Zaharia LI, Galka MM, Ambrose SJ, Abrams SR. 2005. Preparation of deuterated abscisic acid metabolites for use in mass spectrometry and feeding studies. Journal of Labelled Compounds and Radiopharmaceuticals **48**, 435–445.
Zheng L, Otani M, Kanno Y, Seo M, Yoshitake Y, Yoshimoto K, Sugimoto K, Kawakami N. 2022. Seed dormancy 4 like1 of Arabidopsis is a key regulator of phase transition from embryo to vegetative development. The Plant Journal **112**, 460–475.
Zhou Y, Romero-Campero FJ, Gómez-Zambrano Á, Turck F, Calonje M. 2017. H2A monoubiquitination in Arabidopsis thaliana is generally independent of LHP1 and PRC2 activity. Genome Biology **18**, 69.